

..... al mio papà .....



**UNIVERSITA' DEGLI STUDI DI PISA  
FACOLTA' DI MEDICINA E CHIRURGIA**

---

**Corso di Specializzazione in Patologia Clinica**

**Fasting induces Anti-Warburg Effect that Increases  
Respiration but Reduces ATP-Synthesis to Promote  
Apoptosis in Colon Cancer Models**

**Relatore**

Prof.ssa Maria Adelaide Pronzato

**Correlatori**

Dr. Vito Pistoia

Dr.ssa Lizzia Raffaghello

**Candidato**

Dr. ssa Giovanna Bianchi

**Anno Accademico 2014/2015**

# Background

## Cellular metabolism.

Cellular metabolism is the summary of all the biochemical reactions taking place within a cell. Metabolism is organized in sequences of biochemical reactions called pathways. They can be linear sequences of a few reactions, or extensively branched with reactions converging on or diverging from a central main pathway.

Metabolism is divided into two broad categories:

1) catabolism, which is the combination of the pathways that break down large molecules such as polysaccharides, lipids, nucleic acids and proteins into smaller units including monosaccharides, fatty acids, nucleotides, and amino acids, respectively. All these reactions provide energy which is used to drive the synthesis of adenosine triphosphate (ATP). The monomers, released from breaking down polymers, are used to construct new polymer molecules and to maintain cell growth. Examples of catabolic processes include glycolysis, the citric acid cycle (TCA), the breakdown of proteins in order to use amino acids as substrates for gluconeogenesis and the breakdown of fat in adipose tissue to fatty acids (Figure 1).

2) anabolism is the set of pathways that construct molecules from smaller units provided by catabolism. Many anabolic processes are powered by the hydrolysis of ATP. The main function of the anabolic pathways is to synthesize the four classes of macromolecules essential for the cell: polysaccharides, lipids, nucleic acids and proteins. The most important

anabolic pathways are gluconeogenesis, pentose phosphate shunt (PPP), protein and lipid synthesis (Figure 1).

Metabolism is a dynamic process. The cell is continuously degrading and synthesizing molecules and this constant turnover of cellular materials keeps the cell in good condition. Cellular metabolism is the most fundamental level where the dynamic properties of life begin to appear. The complex interactions of different pathways, their regulation, and their organization demonstrate the perfect refinement of the biochemistry of life.

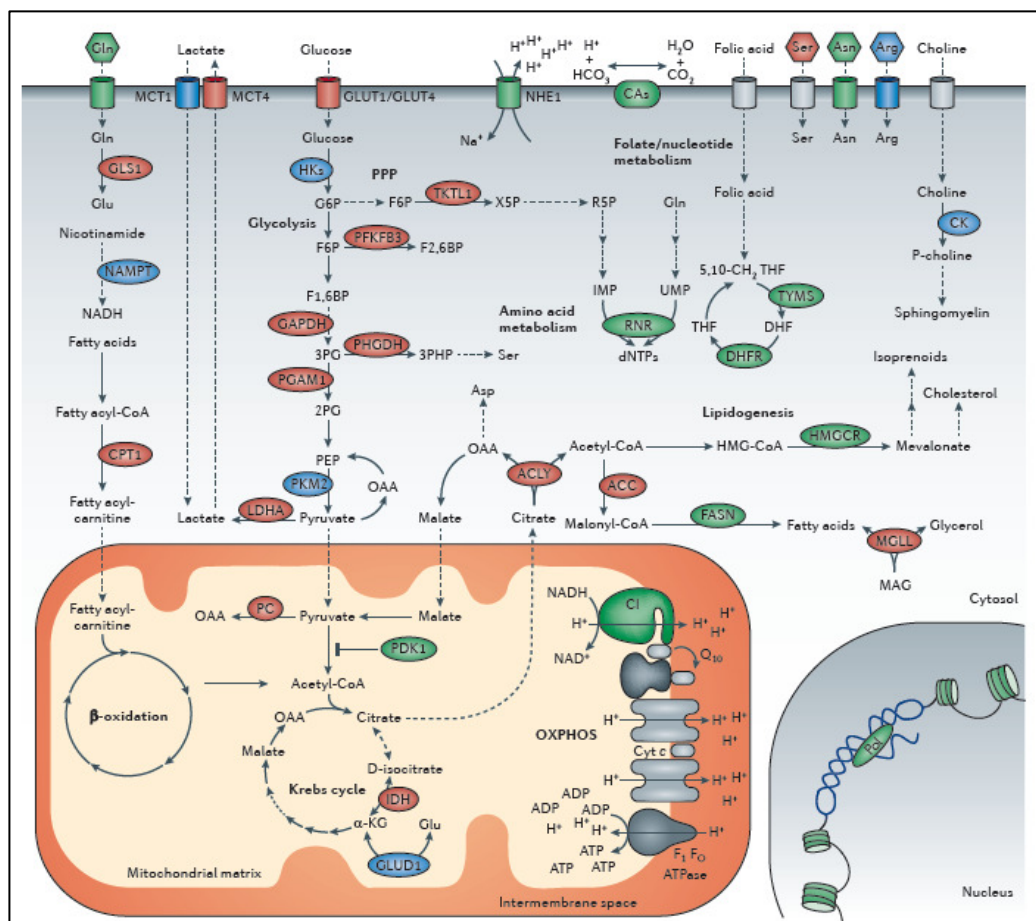


Figure 1. Overview of cellular metabolism

### **The Warburg effect**

Our common knowledge of metabolic pathways is principally based on studies performed on non proliferating cells in differentiated tissues. In normal cells, the metabolism of the basic energy substrates (carbohydrates, proteins, and lipids), generates several metabolic intermediates that are used to synthesize nucleic acids, nonessential amino acids, glycogen, and other biomolecules required for normal body functioning. Since energy is critical to all biologic processes, metabolism partly results in the production of acetyl CoA that is oxidized in the TCA cycle to produce reducing equivalents necessary for energy generation by the respiratory chain. Carbohydrates are broken down to glucose, which is taken up by cells and metabolized via the fundamental biochemical process known as glycolysis. Glucose enters in the cell through specific glucose transporters (GLUTs) (1), which include a large family of plasma membrane proteins (GLUT-1, GLUT-2).

In the cytosol, several enzymes catalyze glycolysis that ends with the production of pyruvate and two molecules of ATP per glucose. Pyruvate enters the mitochondria and is converted to acetyl CoA by pyruvate dehydrogenase (PDH). Acetyl CoA condenses with oxaloacetate (OAA) to form citrate, which is completely oxidized in the TCA cycle to generate reducing equivalents for the respiratory chain. The respiratory chain produces ~34 ATP molecules per glucose, bringing the total number of ATPs produced per complete oxidation of glucose to ~36, which accounts for over 90% of the energy requirements of the normal cell (2). Thus, in normal cellular intermediary metabolism, glycolysis, TCA cycle and respiratory chain activities are tightly linked and regulate.

The most noticeable features of proliferating cancer cells are their ability to uptake huge amounts of glucose and to sustain high rates of glycolysis for ATP generation, independently from oxygen availability. This phenomenon is known as “Warburg effect”, from the name of its discoverer Otto Warburg (Figure 2) (3-5). To explain this event, he firstly hypothesized a defect in mitochondrial respiration as a cause for the increased aerobic glycolysis in tumor cells. However, it was later appreciated that mitochondrial defects are uncommon in malignant cells (6) and that most tumours maintain the capacity for oxidative phosphorylation and they consume oxygen at rates similar to those observed in normal tissues (7). Other explanations consider that glycolysis has the capacity to generate ATP at a higher rate than oxidative phosphorylation and so would be beneficial as long as glucose supplies are not limited. In turn, it has been proposed that glycolytic metabolism derives from an adaptation to hypoxic tumor microenvironment, as it allows for ATP production in the absence of oxygen (8, 9). In addition, enhanced uptake of glucose and its conversion into lactate creates the problem of intracellular acidification and lactate accumulation (10,11). The lactate produced is secreted out of the cells to warrant cancer cell survival and to keep aerobic glycolysis active. Moreover, different studies suggest that extracellular lactate facilitates immune escape, migration, metastasis, tumor vascularization and radioresistance (12-14). The most recent explanation for the switch to aerobic glycolysis by tumor cells, is that proliferating cells have important metabolic requirements that extend beyond ATP. Tumor cells must replicate all of its cellular contents to sustain mitosis. This aspect imposes a large requirement for nucleotides, amino acids, and lipids. During growth, glucose is used to

generate biomass as well as produce ATP whose hydrolysis provides free energy to sustain anabolic pathways (11).

New evidences suggest that the Warburg effect is a strategy, used by cancer cells, not only to face up to multiple urgent requirements simultaneously for growth and proliferation but also to reduce reactive oxygen species (ROS) and therefore oxidative stress.

The Warburg effect has found widespread clinical utility in the imaging of cancer using  $^{18}\text{F}$ -Fluorodeoxyglucose (2-fluoro-2-deoxy- D-glucose – FDG) in positron emission tomography (PET) scans. A glucose analog, 2-fluoro-2-deoxy-D-glucose, is, therefore, taken up at higher concentrations in cells with increased glucose transport such as malignant cells. Intracellular FDG is phosphorylated by hexokinases (HK) to FDG-6-phosphate, which cannot be metabolized further in glycolysis. Thus, FDG-6-phosphate accumulates in the cell and the radioactive isotope fluorine-18 enables imaging of the cell before radioactive decay. The technology is used in the diagnosis, staging, and monitoring of several cancers, including lymphoma, melanoma, and cancers of the colon, breast, and lung (15).

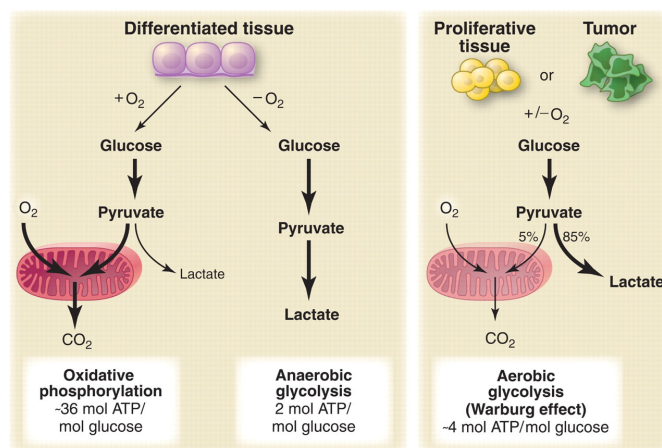


**Figure 2. The Warburg effect**

### **The PI3K/ATK/mTOR pathway.**

Mutations that activate oncogenes or inactivate tumor suppressors can significantly affect activities of metabolic enzymes and have a key role in aerobic glycolysis of cancer. Among oncogenic mutations, hyperactivation of the phosphatidylinositol 3'-kinase (PI3K)/Protein kinase B (AKT)/mammalian target of rapamycin (mTOR) axis initiates a signal transduction cascade that promotes cancer cell growth, survival and metabolism (16, 17).

PI3Ks are a family of lipid kinases that propagate intracellular signaling regulating a wide range of cellular processes. There are three distinct classes of PI3K, but the I<sub>A</sub> PI3Ks is the most implicated in cancer cell growth and survival. Class IA PI3Ks are activated by growth factor receptor tyrosine kinases (RTKs). As shown in figure 3, both insulin and insulin growth factor 1 (IGF1) receptors use the insulin receptor substrate (IRS) family of adaptor molecules to engage class IA PI3Ks, whereas other receptors, such as the platelet-derived growth factor (PDGF) receptor, recruit class IA PI3Ks directly (18). I<sub>A</sub> PI3Ks phosphorylate phosphatidylinositol-4,5-bisphosphate (PIP<sub>2</sub>) on the plasma membrane to generate the second messenger, phosphatidylinositol-3,4,5-trisphosphate (PIP<sub>3</sub>). The accumulation of PIP<sub>3</sub> on the cell membrane leads to the recruitment and the activation of protein with pleckstrin homology (PH) domain known as phosphoinositide-dependent protein kinase 1 (PDK1) which phosphorylates Akt at T308. The full activation of Akt is provided by S473 phosphorylation mTORC2-mediated (Figure 3) (19, 20). Phosphatase and tensin homolog deleted on chromosome 10 (PTEN) by dephosphorylating the 3' position of phosphatidylinositol-3,4,5-trisphosphate (PIP<sub>3</sub>) to phosphatidylinositol 4,5-bisphosphate (PIP<sub>2</sub>), antagonizes the PI3K-



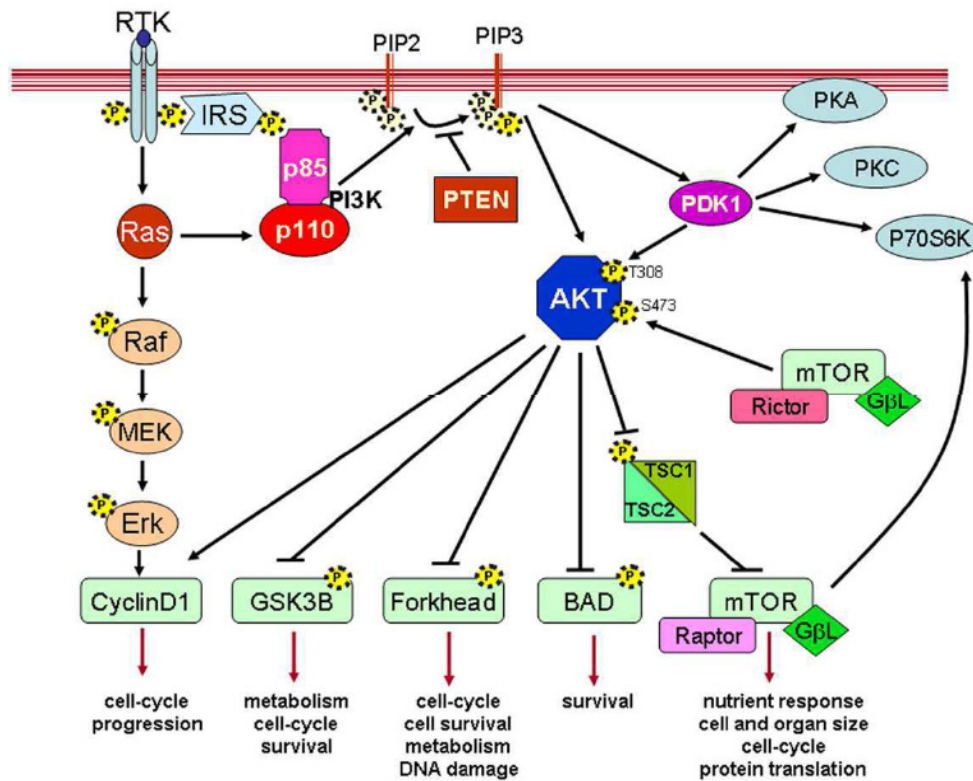
Akt signaling pathway (21). The central biological consequences of Akt activation can be classified into three categories, survival, proliferation, and growth. Moreover, Akt has important effects on tumor-induced angiogenesis that is partly mediated by hypoxia-inducible factor-1 $\alpha$  (HIF-1 $\alpha$ ) and vascular endothelial growth factor (VEGF) (22). Akt has an anti-apoptotic function through BAD-phosphorylation, a member of BCL2 family of proteins that promotes cells death (23). Although Akt inhibits apoptosis through pro-death protease Caspase-9 and forkhead box O transcription factors (FoxO) phosphorylation (24, 25), it can also influence the activity of the pro-apoptotic tumor suppressor p53, through phosphorylation of the p53-binding protein MDM2 (26, 27).

Several studies demonstrated that p53 plays an important role as regulator of metabolism. For example, p53 activates the expression of hexokinase 2 (HK2), which converts glucose to glucose-6-phosphate (G6P). G6P is directed through glycolysis and PPP to produce ATP and to support macromolecules biosynthesis. p53 inhibits the glycolytic pathway by upregulating the expression of TP53-induced glycolysis and apoptosis regulator (TIGAR), an enzyme that decreases the levels of the glycolytic activator fructose-2,6-bisphosphate (28-30).

The cell cycle is regulated by the orchestrated action of cyclin–cyclin-dependent kinase (CDK) complexes and CDK inhibitors (CKIs). Cyclin D1, which is implicated in the G1/S phase transition, is phosphorylated by the cyclin D1 kinase glycogen synthase kinase-3 (GSK3 $\beta$ ) and degraded by the proteasome. Akt directly inhibits GSK3 $\beta$  allowing to Cyclin D1 accumulation and supporting tumor cell proliferation (Figure 3) (31). In addition to its role in

proliferation, there is growing evidence that Akt also affects the synthesis of macromolecules, which results in increased cell mass or size, a process that is enhanced in cancer cells to meet the biosynthetic requirements that are imposed by the augmented degree of proliferation.

The “main character” involved in the PI3K-pathway is mTOR, a serine/threonine kinase that acts as a molecular sensor regulating protein synthesis on the basis of nutrients availability. mTOR exists in two distinct intracellular complexes, mTOR complex 1 and 2 (mTORC1 and mTORC2). mTORC1 is a complex of mTOR with regulatory-associated protein of mTOR (raptor), LST8 and Akt1 substrate 1 (AKTS1). Unlike mTORC2, mTORC1 is effectively inhibited by rapamycin and its analogues (32). mTORC1 phosphorylates p70 S6 kinase and 4E-binding protein 1 (4EBP1), 4EBP2 and 4EBP3. These phosphorylation events imply the increased translation of mRNAs that encode many cell cycle regulators (33). mTORC1 activity is controlled by the tuberous sclerosis 1 (TSC1)–TSC2 complex which functions as a GTPase-activating protein (GAP) for the small G protein Ras homologue. TSC2 is directly phosphorylated in response to growth factor signalling such as PI3K–Akt and ERK–Rsk signaling and energy homeostasis through AMP-activated protein kinase (AMPK) (34). Akt1 stimulates aerobic glycolysis by promoting the synthesis and incorporation of GLUT1 into the plasma membrane (35-37); by stabilizing the association between HK2 and mitochondria, hence increasing its enzymatic activity (38) and by activating 6-phosphofructo-2-kinase/fructose-2,6-biphosphatase 3 (PFKFB3) (39). In addition, Akt1 stimulates lipid biosynthesis by increasing the activity of ATP citrate lyase (ACLY).



FONTE: Amancio Carnero and Jesus M.Paramio. Front. Oncol., 23 September 2014 | doi: 10.3389/fonc.2014.00252

Figure 3. Molecular mechanism of the PI3K/Akt/mTOR pathway

### ROS: a double edge sword

The term reactive oxygen species concerns several molecules derived from oxygen that have accepted extra electrons and can oxidize other molecules (40). Specificity in ROS signalling takes advantage of the distinct biological properties of each oxidant species, which include their chemical reactivity, stability, and lipid diffusion capabilities. As shown in Figure 4,  $O_2^-$  is generated by the cytosolic NADPH oxidases (NOXs) (41, 42) through the one-electron reduction of  $O_2$  occurring in mitochondrial electron transport chain (ETC) complexes I, II, and III (43, 44).

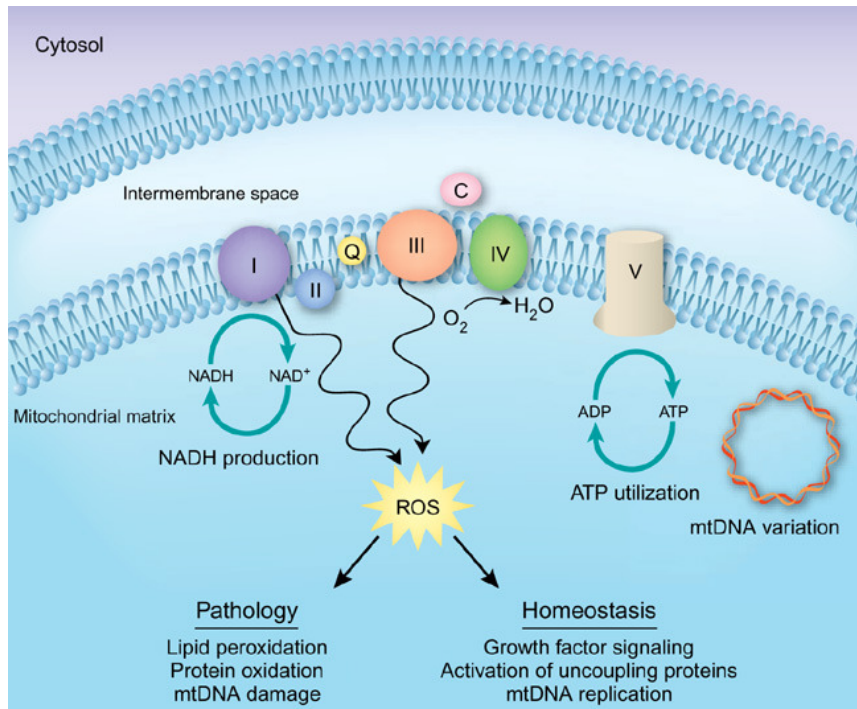


**Figure 4. The generation and consequences of ROS in mitochondria.**

Cytosolic  $O_2^-$  is rapidly converted to  $H_2O_2$  by the enzymatic activity of superoxide dismutase 1 (SOD1).  $O_2^-$  generated by the mitochondrial ETC is released into the matrix where it is quickly dismutated to  $H_2O_2$  by superoxide dismutase 2 (SOD2). Complex III-generated  $O_2^-$  is also released into the intermembrane space where it can traverse through voltage-dependent anion channels into the cytosol and be converted into  $H_2O_2$  by SOD1. In addition,  $H_2O_2$  is produced in the endoplasmic reticulum (ER) as an end product in numerous peroxisomal oxidation pathways such as in the  $\beta$ -oxidation of very long-chain fatty acids, and by a wide range of enzymes including cytochrome P450 (45). A well known mechanism of redox signalling involves  $H_2O_2$ -mediated oxidation of cysteine residues within proteins. Cysteine residues exist as a thiolate anion (Cys-S<sup>-</sup>) at physiological pH and are more susceptible to oxidation compared with the protonated cysteine thiol (Cys-SH). During

redox signalling,  $H_2O_2$  oxidizes the thiolate anion to the sulfenic form (Cys-SOH), causing allosteric changes within the protein. This event alters protein function. The sulfenic form can be reduced to thiolate anions by the disulfide reductases thioredoxin (Trx) and glutaredoxin (Grx) to return the protein function to its original state. Hence, the oxidation of cysteine residues within proteins could represent a mechanism to reverse signal transduction mechanism. Nonetheless, higher level of  $H_2O_2$  causes oxidative stress, damaging proteins. Therefore, cells have professional enzymes dedicated to prevent the build-up of intracellular  $H_2O_2$  such as peroxiredoxins and glutathione peroxidases.

Cancer cells constitutively activate growth factor pathways to sustain cellular growth and proliferation (Figure 5). Consequently, tumor cells show an “hyper-metabolism” linked to an abnormal generation of ROS from mitochondria and the endoplasmic reticulum, which cause genomic instability (46). Moreover, the high levels of ROS activate signalling pathways proximal to the mitochondria to promote cancer cell proliferation and tumorigenesis (46). In fact, ROS can i) inhibit phosphatases such as PTEN, to dysregulate PI3K signalling resulting in increased Akt signalling and enhanced proliferation and survival (47) ii) over express HIFs, regulating metabolic adaptation to hypoxia and the expression of pro-angiogenic genes such as vascular endothelial growth factor (VEGF) (48) iii) activate MAPK pathway and NF- $\kappa$ B to enrich the antioxidant counterparts to avoid ROS cell death-mediated (Figure 5) (49).

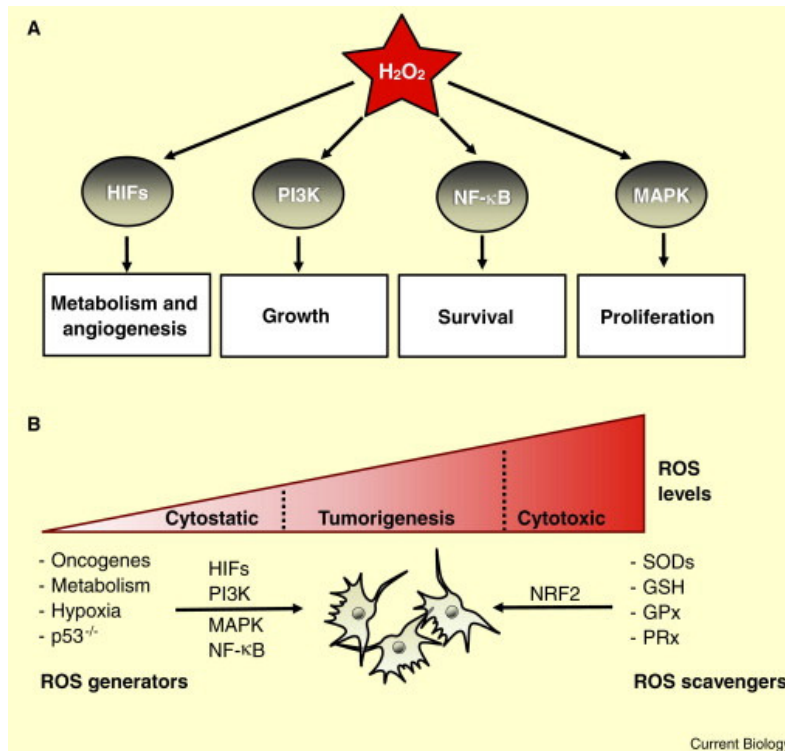


**Figure 5. Signaling pathway activated by ROS.**

Indeed, ROS are also a major contributor to oxidative damage (50). Thus the cellular levels of ROS must be balanced in order to promote cancer cell growth and proliferation without causing severe oxidative damage and cell death. ROS production in cancer cells is elevated due to oncogenic stimulation and increased metabolic activities (51). The Warburg effect, which leads to the production of NADPH and thus a proper redox status, becomes an important survival mechanism for cancer cells. In fact, one of the most important features of the Warburg effect is the switch of the isoform of pyruvate kinase (PK), which catalyzes the conversion of phosphoenolpyruvate (PEP) to pyruvate as the last step of glycolysis. Many tumor cells use the M2 isoform of pyruvate kinase (PKM2) instead of the M1 isoform of the enzyme (PKM1) as normal tissues do (Figure 6) (52-54). PKM2 has an enzymatic activity lower than PKM1. This event leads to the upregulation of glucose uptake and

accumulation of earlier glycolytic intermediates, such as PEP. This, in turn, triggers PPP producing more NADPH which reduces ROS. In addition, ROS and PKM2 form a negative feedback loop to maintain ROS in a tolerable and functional range. Since ROS contribute to mitogenic signalling, reducing intracellular ROS levels could represent a new strategy to inhibit cancer growth. Contrary to the expected results, in several large-scale studies, it has been demonstrated that supplementation of antioxidant molecules increased the risk of cancer (55, 56). A more promising strategy seems to be blocking antioxidant pathways or stimulating ROS production. Both methods lead to the accumulation of toxic levels of intracellular ROS pushing cells to die (57) (Figure 6).

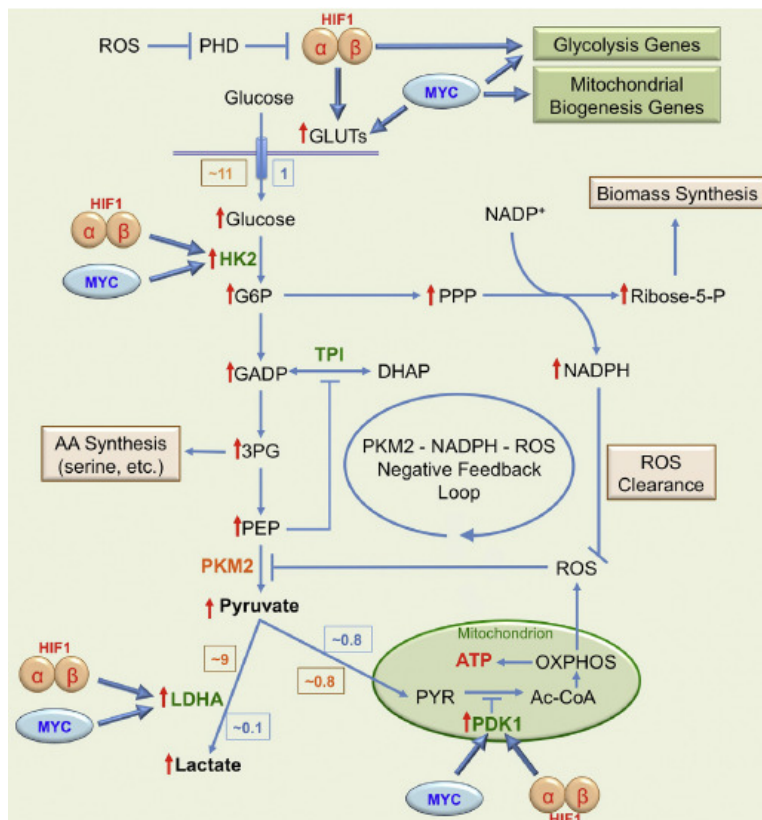


Figure 6. Linking ROS to the Warburg effect.

### **Targeting the Warburg effect to treat cancer.**

Some of the most important features of the Warburg effect are: (i) increased expression of GLUTs and increased glucose uptake; (ii) increased PPP-catalyzed NADPH production; (iii) altered activities of glycolytic enzymes and (iv) increased lactate production. Some of these features could potentially be targeted to develop new strategies for cancer therapy.

Up to 90% of all cancers are characterized by upregulation of GLUT expression and glucose metabolism. At least, 12 GLUTs have been identified, but the major role in cancer have been associated to GLUT1 and GLUT2 (58). Several *in vivo* studies demonstrated that GLUT1 inhibition represents a compelling anticancer strategy (59-61). Furthermore, drugs targeting glycolytic enzymes, in particular HK and LDH inhibitors, could represent good strategy to suppress tumorigenesis. These agents could inhibit tumor growth by decreasing metabolic precursors for glycolysis, slowing down synthesis of biomass and reducing equivalents and causing ROS dysregulation.



## ***Calorie restriction***

### **Definition**

In the last century life expectancy at birth has markedly increased from about 45 years at the beginning of the 20th Century to about 77 years today in many developed countries, including Western Europe, USA, Canada, Japan, Australia, and New Zealand (62). However, the increase in life expectancy does not go hand in hand with the quality as evidenced by the rising burden of chronic diseases, including abdominal obesity, type 2 diabetes, chronic lower respiratory disease, Alzheimer's disease, heart and cerebrovascular diseases, and cancer (63). Almost 80% of older adults (+65 years) have at least one of the above mentioned chronic diseases, and 50% have at least two chronic diseases (Figure 7). The main risk factors for the above mentioned chronic diseases are associated to i) the consumption of foods high in caloric intake but devoid of nutrients (e.g., vitamins, phytochemicals), ii) physical inactivity and iii) smoking (64).

Aging is a biological and psychological process, not due to illness, occurring in all individuals after maturity which gradually reduce the ability of the organism to adapt to stress and to maintain the homeostasis. Aging depends on genetic factors for 30% and on the environment for 70%. It is irreversible and produces an increased susceptibility to the disease. Oxidative damage to cell components, caused by an imbalance between ROS and antioxidant systems, is considered the most important player in causing this phenomenon. Indeed, aging is accompanied by progressive accumulation of oxidative damage in many tissues, including the peripheral and central nervous systems (PNS, CNS) (65-68).

Biogerontology studies performed in the past decade indicate that dietary modification or genetic manipulations extend longevity by producing a shift to a maintenance mode characterized by enhanced stress resistance. The longevity and stress-resistance regulation can be obtained by mutations that decrease the activity of nutrient-signaling pathways or by reducing calorie intake by at least 30%, without malnutrition, a strategy called dietary or calorie restriction (DR/CR) (69, 70). Calorie restriction triggers highly conserved survival mechanisms that enhance the protection of organisms ranging from bacteria, yeast, worms, flies, and mice, to non-human primates against various types of stress and/or disease including diabetes, cardiovascular disease and cancer. This counterintuitive effect is mediated in part by the reduction of conserved nutrient-signaling pathways that include several mitogenic components, especially the IGF-I receptor and its downstream effectors (69, 71-74).

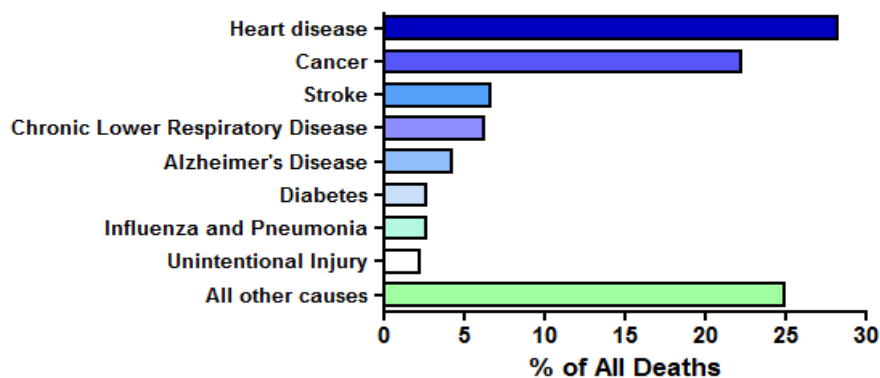


Figure 7. Causes of death in adults aged 65 years or older

### **Calorie restriction in model organism.**

CR remains the most robust non-genetic nutritional experimental intervention for life extension in many species, including yeast, fruit flies, nematodes, fish, rats, mice, and monkeys (75). Invertebrate model organisms, such as yeast, *Caenorhabditis elegans* (*C. elegans*) and *Drosophila*, are largely exploited to understand the molecular anti-aging mechanisms of CR.

Mutations involved in the extension of lifespan were first discovered in *C. elegans*, and led to the discovery of the role of the insulin/Igf-like (IIS) axis in aging (76).

The impairment of IIS pathway by CR, in yeast *Saccharomyces cerevisiae*, *C. elegans* and in *Drosophila* causes the down regulation of PI3K/mTOR/Akt pathway activity (Figure 8). As consequence, it is possible to observe the activation or inhibition of different transcription factors, (such as Forkhead FoxO transcription factor, eIF4E-binding proteins (4E-BP) involved in i) cellular stress-response ii) detoxification of xenobiotics and free radicals and iii) protein translation (77, 78). However, the metabolic, anatomical, physiological and lifespan differences between these invertebrate model organisms and the mammalian systems are enormous.

Rodents provide an extremely valuable and flexible animal model in which to determine the ability of CR to extend maximum lifespan and healthspan in a mammalian system.

Mutation in the growth hormone receptor (GHR) and mutations that cause GH/IGF-I deficiency represent the genetic interventions causing the longest life span extension in mammals (79).

In agreement with the results in worms and flies discussed earlier, inhibition of the mTOR pathway beginning at 600 days of age extends median and maximal lifespan of mice (80) and the deletion of ribosomal S6 protein kinase 1 (S6K1), a component of the mTOR signaling pathway, leads to increased life span and resistance to age-related pathologies, including bone, immune, and motor dysfunction and insulin resistance (81). The connection between signal transduction pathways and stress resistance in mammals may involve transcription factors including the orthologs of the anti-aging transcription factors described in yeast, worms and flies (Figure 8).

CR, without malnutrition, in mice and rats has been clearly demonstrated to increase both average and maximal lifespan by preventing or delaying the occurrence of a wide range of chronic diseases and by inhibiting spontaneous, chemically- and radiation-induced cancer (82). CR has also been shown to prevent or delay the occurrence of chronic nephropathies and cardiomyopathies, diabetes, autoimmune and respiratory disease (75) and decreases neurodegeneration in the brain of animal models of Alzheimer disease, Parkinson disease, Huntington disease, and stroke (83, 84). Similar to rodents, in monkeys CR determines a significant reduction of age-related diseases such as cancer and cardiovascular disease. Moreover, CR protects monkeys against obesity and diabetes and stimulates immune system function (85).

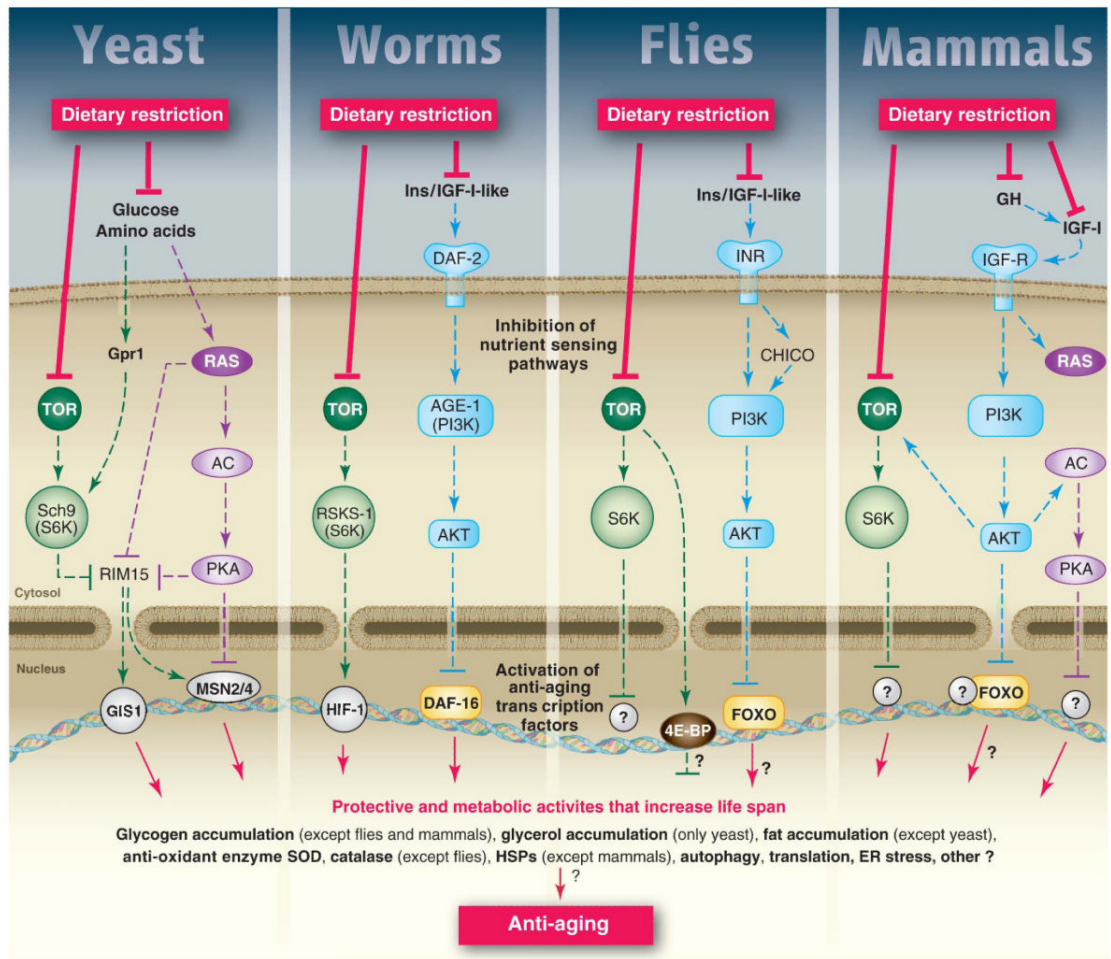


Figure 8. A model for the conserved nutrient signalling pathways that regulate longevity in various organisms and mammals

### **Calorie restriction in humans.**

In humans, CR refers only to a state in which energy intake is sufficiently low to achieve or maintain a low-normal body weight status (i.e., body mass index < 21 kg/m<sup>2</sup>) without causing malnutrition (i.e., adequate intake of proteins and micronutrients) (64). Epidemiological studies, conducted on the inhabitants of Okinawa (Japan), which mainly consume vegetables and fish with a daily calorie intake 40% less in comparison to that of a Japanese or US resident (86), showed that Okinawans have a delay or sometime an escape of chronic diseases of aging including dementia, cardiovascular disease and cancer.

Since 1991 to 1993, in Arizona, four men and four women were enrolled in a controlled study called Biosphere 2. They lived for 18 months in a close ecosystem, experiencing a forced decrease in calorie intake. The reduced energy intake associated to a highly physical activity lowered body weight, blood pressure, blood glucose, insulin, cholesterol, triiodothyronine and white blood cells (87).

Similar results were obtained by the Calorie Restriction Society, a group composed by volunteers, who had been eating about 1800 kcal/day for an average of 6.5 years (30% less calories than age-matched and sex-matched volunteers consuming a typical Western diet) (88). Indeed, serum total cholesterol, low density lipoprotein cholesterol (LDL), triglycerides, fasting glucose, fasting insulin but not HDL-C, were significantly lower in the CR group than in the US diet control group. Moreover, the CR group resulted more protected against atherosclerosis and hypertension and diabetes (89).

Significant differences in the metabolic and physiologic effect of CR between mice and humans have been described. In rodents, CR without protein restriction induces a 20–40% reduction in the level of IGF-1 while in humans, severe CR without reduction of protein intake does not reduce serum IGF-1 and IGF-1/IGFBP-3 concentrations. On the other hand, severe reduction of protein intake could have a negative impact on human health. These findings suggest that it is very important to understand the right rate of daily protein intake to protect whole body against stress and disease without side effects (90-92).

### **Calorie restriction: molecular and metabolic aspects**

Several mechanisms have been proposed to explain the biological basis of the CR life-prolonging and anti-aging actions. It is not easy to obtain clear and supported by evidence answers, but it is certain that CR implicates a combination of metabolic, physiological and cellular adaptations to CR itself.

One of most potent effects of CR is its ability to suppress GH/IGF-1 axis. GH directly regulates the production of IGF-I, which is the major mediator of the growth effects of GH (79). In humans, IGF-I levels decrease dramatically in response to short-term starvation (36–120 hours) despite increased GH secretion (93, 94). Notably, the RAS/RAF/MAPK and the PTEN/PI3K/Akt pathways, which mediate suppression of apoptosis and contribute to proliferation and cell growth, can be down regulated possibly by reducing IGF-I (95). These pathways are important in determining the sensitivity of tumors to CR, and specific mutations have been shown to confer cancer resistance to CR (96). In addition to alteration in IGF-1 signaling, alterations of the insulin

and mTOR/Akt/S6K pathways appear to contribute to the effect of CR on longevity.

Another very potent effect of CR is to reduce ROS production and to maintain the redox balance. ROS are produced by different cellular sources, such as cyclooxygenase (COX), which is involved in inflammation by producing prostaglandins, prostacyclin and thromboxane. CR is known to inhibit COX activity and ROS related production. COX activity is related to the transcription factor NF- $\kappa$ B activity which is responsible for the transcription of many pro-inflammatory proteins like TNF- $\alpha$ , IL-1, IL-2, and IL-6; chemokines; adhesion molecules (AMs), including ICAM-1, VCAM-1, and enzymes such as inducible NO synthase (iNOS) and COX-2. However, contradictory results were obtained about CR effect on NF- $\kappa$ B activity (97, 98).

Finally, CR plays an important role in neuroendocrine adaptations, that have been hypothesized to be involved in the anti-aging effects of CR. Indeed, CR causes: i) reduction of thyroid hormones and catecholamines that regulate thermogenesis and cellular metabolism (ii) decrease of testosterone, estradiol, insulin, leptin which are anabolic hormones and (iii) increase of glucocorticoids, adiponectin and hormones that suppress inflammation (100).



**Short-term-starvation, differential-stress-resistance and cancer.**

Cancer is a complex multistage disease associated with accumulation of multiple DNA mutations that cause a deregulation of cell proliferation and differentiation, loss of normal tissue organization, and eventually tissue invasion and dislocation to distant sites (Figure 9) (101). DNA damage, which occurs continuously in both the dividing and non dividing cells of the human body, and can increase after exposure to exogenous genotoxic carcinogens, can be prevented or repaired by endogenous protective small molecules and enzymes.

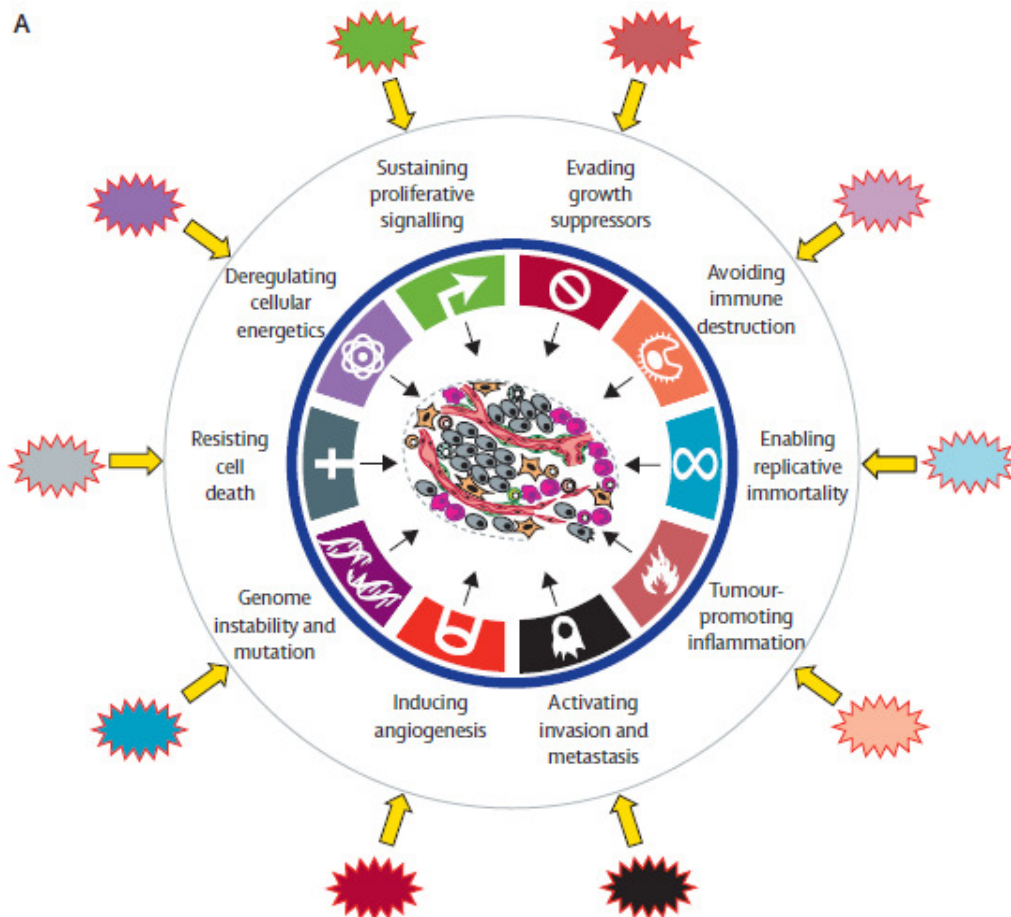


**Figure 9. Hallmarks of cancer**

However, these detoxification and repair systems might fail, particularly in environments that promote cell proliferation and inhibit cell apoptosis, but also in non-dividing cells in which the opportunity for repair might be limited. Accumulation of multiple DNA mutations in critical genes (i.e. oncogenes or tumor suppressor genes) of particular cells, if not properly controlled through induction of senescence or apoptosis, can lead to uncontrolled cell proliferation and progressive malignant transformation (82). Epidemiological studies have shown a significant association between chronic energy imbalance, which promotes hypertrophy of adipose tissue, reduced adiponectin production, insulin resistance and compensatory hyper-insulinemia, and increased risk of cancers (102, 103) .

Chemotherapy has established itself as one of the pillars of cancer treatment and extend survival in patients diagnosed with a wide range of malignancies. However, side effects caused by toxicity to normal cells and tissues limit chemotherapy dose intensity, which may compromise efficacy. Thus, reduction of undesired toxicity by selective protection of normal cells without compromising the killing of malignant cells represents a promising strategy to enhance cancer treatment. In this connection, Valter Longo and his co-workers demonstrated that non-malignant cells can be induced to turn into a self protection mode by conditions of STS (105). In healthy cells, STS was found to activate protective metabolic pathways that confer resistance to oxidative stress, such as that inflicted by anticancer agents, an effect termed “differential stress resistance” (DSR) (Figure 10).

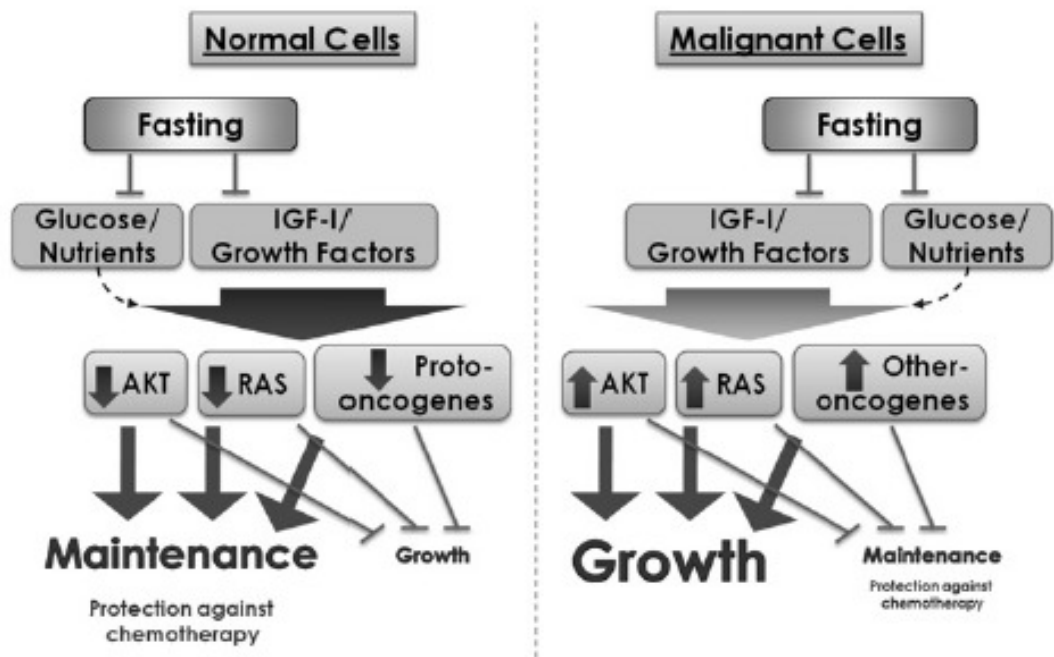


**Figure 10. Molecular mechanisms at the basis of the Differential-stress-resistance**

In striking contrast, cells expressing activated oncogenes are unable to turn on the protective response due to uncontrolled activation of growth promoting signaling cascades and become even more sensitive to anticancer agents (“differential stress sensitization”, DSS). Accordingly, in experiments using mouse models of human cancer, fasting specifically augmented the levels of oxidative stress and sensitivity to oxidative damage in response to chemotherapeutic agents in cancer cells and these effects were accompanied by DNA damage and apoptosis. Notably, some of the systemic changes induced by fasting, such as hypoglycemia and a marked reduction in the circulating levels of IGF-1, are also credited with anticancer activity *in vivo*.

The first clinical experience with fasting in patients receiving chemotherapy indicates that this dietary intervention is feasible, safe and significantly reduces common side effects induced by chemotherapy (Figure 11) (107,108).

Furthermore, in those patients whose cancer progression could be assessed, fasting does not prevent the chemotherapy-induced reduction of tumor volume or tumor markers (107). The discovery that STS may not only alleviate the side effects of chemotherapy, but also increase its effects on cancer cells has recently attracted further attention to this approach amongst physicians and patients, and several pilot trials (NCT01304251, NCT01175837, NCT00936364, NCT01175837) are currently exploring fasting in combination with chemotherapy in humans.

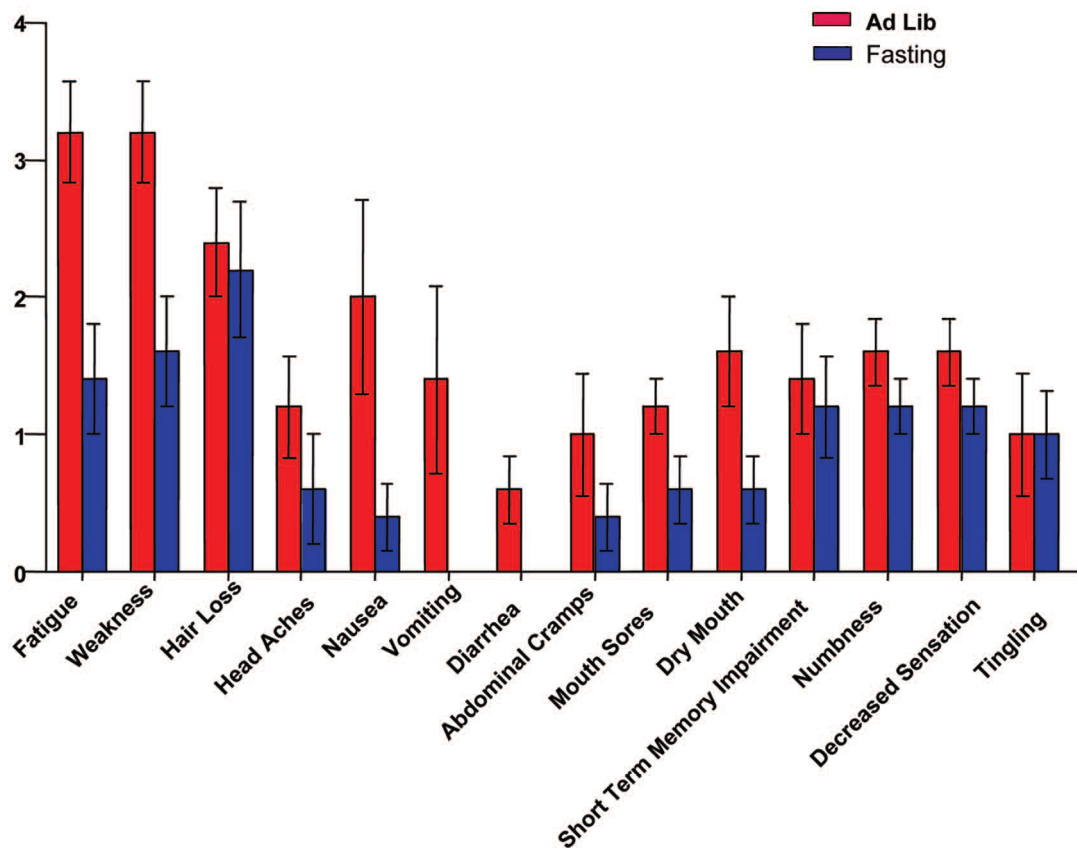


Figure 11. Self reported side effects after chemotherapy with or without fasting

## **Summary of the study**

Tumor chemoresistance is associated with high aerobic glycolysis rates and reduced oxidative phosphorylation, a phenomenon called “Warburg effect” whose reversal could impair the ability of a wide range of cancer cells to survive in the presence or absence of chemotherapy. In previous studies, Short-term-starvation (STS) was shown to protect normal cells and organs but to sensitize different cancer cell types to chemotherapy but the mechanisms responsible for these effects are poorly understood. We tested the cytotoxicity of Oxaliplatin (OXP) combined with a 48hour STS on the progression of CT26 colorectal tumors. STS potentiated the effects of OXP on the suppression of colon carcinoma growth and glucose uptake in both *in vitro* and *in vivo* models. In CT26 cells, STS down-regulated aerobic glycolysis, and glutaminolysis, while increasing oxidative phosphorylation. The STS-dependent increase in both Complex I and Complex II-dependent O<sub>2</sub> consumption was associated with increased oxidative stress and reduced ATP synthesis. Chemotherapy caused additional toxicity, which was associated with increased succinate/Complex II-dependent O<sub>2</sub> consumption, elevated oxidative stress and apoptosis .

These findings indicate that the glucose and amino acid deficiency conditions imposed by STS promote an anti-Warburg effect characterized by increased oxygen consumption but failure to generate ATP, resulting in oxidative damage and apoptosis.

**Keywords:** Fasting; Warburg effect; colon cancer; oxidative phosphorylation; glucose uptake

## Introduction

Tumor cells are characterized by high glucose uptake and lactate production regardless of oxygen concentration, a phenomenon known as the “Warburg effect” (11). The metabolic shift toward the Warburg effect confers bioenergetic and biosynthetic advantages to proliferating cells by increasing non-oxidative ATP production and generating metabolic intermediates from glucose important for cell growth (109). Glutamine represents an additional metabolite catabolized by tumor cells and utilized for biosynthetic processes (110). Aerobic glycolysis and glutaminolysis contribute to the chemoresistance of cancer cells (111) through: i) increased lactate production and export, ii) elevated NADPH limiting DNA oxidant drug effectiveness, and iii) decreased oxidative phosphorylation (OXPHOS) rate leading to reduced reactive oxygen species (ROS)-mediated DNA damage (112-114) (115). Therefore, strategies inhibiting glycolysis and glutaminolysis and promoting OXPHOS in order to delay tumor growth and overcome drug resistance are being investigated (116-118). The return of cancer cells to the normal respiratory mode maintained by normal cells could also promote cancer cell death if the respiration was accompanied by electron leakage and superoxide generation (119, 120), leading to cellular damage and apoptosis (121, 122).

In mice, two day cycles of water only fasting (short term starvation, STS) cause a generalized glucose and amino acid reduction/deficiency, which protects normal but not tumor cells against chemotherapy-mediated cytotoxicity (105), and induces potent chemosensitizing effects in many tumors (123, 124).

Preliminary clinical data indicates that in cancer patients fasting is not associated with major side effects and may reduce several of the side effects

associated to chemotherapy (107) including a decreased toxicity to lymphocytes (125). These pre-clinical and preliminary clinical results served as the foundation for randomized trials to test the safety and efficacy of fasting cycles on the effect of chemotherapy on both normal and cancer cells (NCT01304251, NCT01175837, NCT00936364, NCT01175837).

However, the molecular mechanisms responsible for the chemosensitizing effects of fasting and STS on cancer cells remain poorly understood (126) (123).

Here, using both *in vitro* and *in vivo* colon carcinoma models, we show that STS exerts an anti-Warburg effect driving tumor cells from a glycolytic mode into an uncoupled OXPHOS which promotes increased ROS generation and apoptosis. These effects are enhanced by chemotherapy treatment.

## Results

### **Effects of fasting cycles and chemotherapy on colon carcinoma growth and glucose consumption in vivo**

We investigated the effect of STS +/- chemotherapy on glucose metabolism in CT26 colon carcinoma cells in mice by micro-PET analyses. As previously described (105, 123), 48-hour of STS induced a significant body weight loss and serum glucose reduction. Analysis of tracer uptake by the tumor showed a differential response to the treatments (Figure 12A-C). After the first cycle, STS was as effective as OXP in reducing the average tumor glucose consumption (Figure 1C). However, the lowest values were achieved by STS+OXP (Figure 12A-C). Monitoring of tumor progression during multiple cycles revealed that average tumor metabolism was inhibited similarly by the first and second STS

treatments (Figure 12C). Chemotherapy induced only a transient reduction of the lesion metabolic rate after its first application. By contrast, average glucose consumption remained significantly lower in STS+OXP-treated mice (Figure 12C).

The metabolic response to treatment was paralleled by an evident effect of STS on cancer growth, mostly during the fasting and not the post-fasting period (Figure 12D). The transient effect of STS on tumor growth was repeatable. OXP instead showed a deceleration in cancer growth which was enhanced by STS (STS+OXP) (Figure 12D). The additive effect of STS+OXP was also evident when total cancer glucose consumption rate was measured (tumor glucose metabolism/gr/min x total tumor volume). After both cycles, this glucose consumption rate was much lower in either STS- or OXP-treated mice but was lowest in STS+OXP-treated mice compared to that in untreated mice (STS+OXP vs STS 1° cycle P=0.05; STS+OXP vs OXP 1° cycle P=0.03; STS+OXP vs OXP 2° cycle P=0.01) (Figure 12E). In summary, these results indicate that STS enhances the toxicity of chemotherapy to colon cancer cells, resulting in decreased glucose consumption rates.



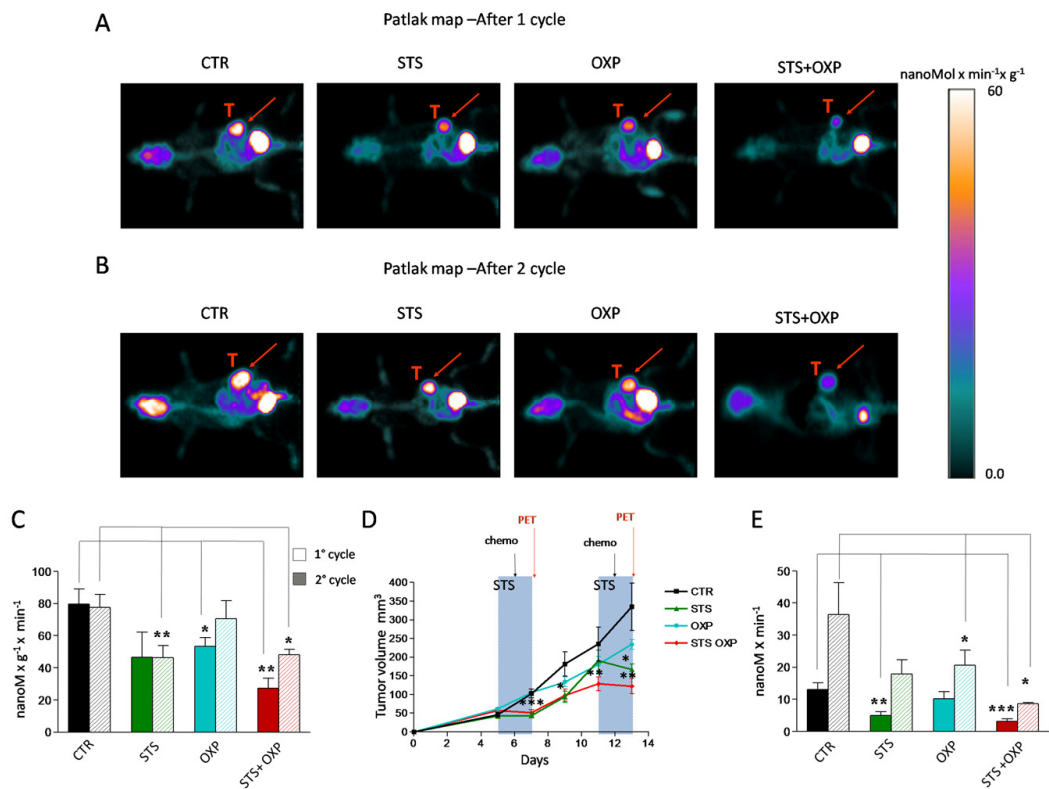


**Figure 12. *In vivo* effect of fasting cycles in combination with chemotherapy on tumor glucose consume and cancer growth.**

CT26 cells were subcutaneously inoculated in the fat pad of BALB/c mice (200.000 cells/mouse). Five days after tumor cell inoculum, the mice were starved or maintained on the ad lib standard diet for 48 hours and treated with Oxaliplatin (OXp) (10 mg/Kg). After 1 week, the treatment was repeated. All mice were imaged after the first and the second cycle of therapy by a dedicated micro-PET system.

Panel A shows the Patlak-map of a representative mouse for each group after the first cycle of treatment.

Panel B shows the Patlak-map of a representative mouse for each group after the second cycle of treatment. Red arrows indicate the tumor mass.

Panel C shows the cancer glucose consumption expressed as nMol x min<sup>-1</sup> gr.

Panel D shows the tumor volume expressed as mean value ± SD. Groups of experiments include: control (black), STS (green), OXp (light blue), and STS+OXp (red).

Panel E shows the total cancer glucose consumption expressed as nMol x min<sup>-1</sup>.

**In vitro effects of STS and chemotherapy on viability and metabolism of colon carcinoma cells**

We investigated the *in vitro* effects of STS on a panel of colon carcinoma cell lines grown under normal or conditions mimicking starvation (123) for 48 hours. One day after STS, the cells were treated with OXP. STS and OXP showed additive cytotoxic effects in all the cell lines (Figure 13A). FDG uptake paralleled viability response since it was reduced by a similar degree by each single stressor, although the greatest impairment occurred in response to STS+OXP (Figure 13B). These results confirm the *in vivo* results and support the use of the *in vitro* paradigm to model the effects of STS in mice.

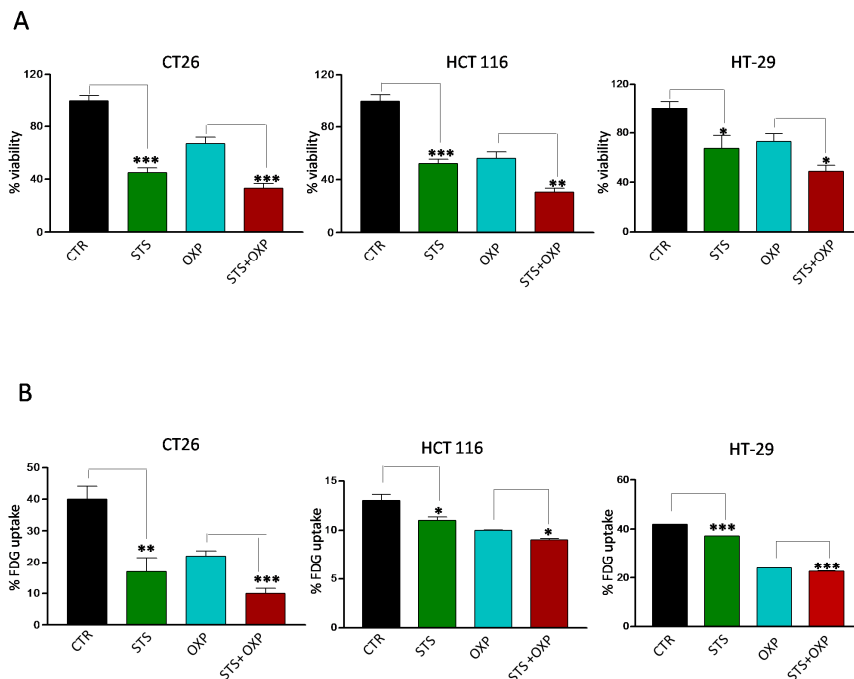


**Figure 13. Effects of STS in combination with chemotherapy on viability and glucose uptake by colon carcinoma cells.**

Tumor cells were cultured in with either low glucose (0.5 g/l) and 1% serum (*in vitro* STS) or the standard glucose levels (1.0 g/l) and 10% serum (control) for 48 hours. Then, cells were incubated with 40  $\mu$ M oxaliplatin (OXP) for 24 hours.

Panel A shows cell viability of different colon carcinoma cell lines (CT26, HCT 116 and HT-29) as determined by Trypan Blue Assay.

Panel B shows <sup>18</sup>F-Fluorodeoxyglucose (FDG) uptake by different colon carcinoma cells (CT26, HCT 116 and HT-29). Tumor cells were incubated with FDG at 37 KBq/ml for 60 minutes. FDG retention was measured as the ratio between bound and total radioactivity.

Data are expressed as percentage of viable cells  $\pm$  SD. P value was calculated using unpaired t-test with Welch's correction. \*: P<0.05; \*\*: P<0.01; \*\*\*: P<0.001.

### **Starvation and chemotherapy differentially regulate proliferation and metabolic enzymes in colon carcinoma cells**

Because CT26 cells displayed the greatest sensitivity to STS in terms of viability and metabolic response (Fig. 14A-B), we selected these cells to measure key mediators of proliferation and glucose metabolism in the PI3K-AKT pathway (PI3K, Phosphatase and Tensin Homolog (PTEN), 3-Phosphoinositide Dependent Kinase 1 (PDK1) and AKT). The effect of STS on metabolism was also evaluated by measuring GLUT1 and GLUT2 (both involved in glucose uptake) and the glycolytic enzyme HKII, PFK, Pyruvate Kinase (PK), and Lactate Dehydrogenase (LDH) expression and enzymatic activity. STS and in particular STS+OXP down-regulated the expression of PI3K/p110 (STS vs CTR: 81%; STS+OXP vs CTR: 48%), phospho-PDK1 (STS vs CTR: 57%; STS+OXP vs CTR: 84%) and phospho-AKT (STS vs CTR: 75%; STS+OXP vs CTR: 58%) and up-regulated PTEN expression (STS vs

CTR: 122%; STS+OXP vs CTR: 121%) (Fig. 3A). Notably, the latter effects matched well the effects of the treatments on CT26 proliferation (Figure 15).

The effects of STS on proteins involved in glucose transport and metabolism was even more evident: STS induced a profound reduction in GLUT1 (STS vs CTR: 15%), GLUT2 (STS vs CTR: 40%), HKII (STS vs CTR: 74%; STS+OXP vs CTR: 48%), PFK1 (STS vs CTR: 74%; STS+OXP vs CTR: 48%), PK (STS vs CTR: 64%; STS+OXP vs CTR: 66%) protein expression, particularly in combination with chemotherapy (Fig. 14A).

HK II catalytic function was reduced by all treatments (Figure 14B) but its intracellular localization was also affected. Immunofluorescence analysis showed a re-localization of HK II from the mitochondrial membrane into the cytosol, particularly after STS+OXP treatment (Figure 14C). Glucose metabolism impairment was further aggravated by the concomitant reduction of PFK (Figure 14D), PK (Figure 14E) and LDH (Figure 14F) activity caused by all treatments. STS-associated impairment of enzymes involved in glucose metabolism was confirmed by the analysis of extracellular lactate concentration, which was markedly reduced by STS alone or in combination with OXP (Figure 14G).

The STS-mediated reduction of glucose catabolism and expression of transport enzymes is consistent with the reduced levels of glucose caused by STS but also with the possibility that STS conditions promote a Warburg reversing effect .

**Expression of glycolytic and glutaminolytic enzymes in response to STS and chemotherapy**

The transcriptome and proteome of STS- and OXP-treated CT26 cells were analyzed by oligonucleotide micorarrays and Label Free Quantitation (LFQ) on High Resolution/Mass Accuracy Liquid Chromatography Tandem Mass Spectrometry (HR/MA LC MS/MS), respectively. Figure 14H shows a heat map of proteins involved in glycolysis and glutaminolysis. The down-regulation of glycolytic enzymes was observed in STS-treated CT26 cells (Figure 14H), with or without OXP treatment. This down-regulation is most likely due to an effect of STS at the transcriptional level since the expression profiles of STS-treated cells show a clear down-regulation of the genes encoding these enzymes (Figure 14I). At the gene expression level, OXP-treated cells also show reduced expression of glycolysis genes but this effect is more evident in STS+OXP-treated cells (Figure 14I). STS also reduced both glutaminase (Gls) mRNA and protein levels. In contrast, the expression of the glutamine transporter Slc1a5 was reduced only at the protein level (Figure 14H-I). The combination of STS+OXP reduced protein and mRNA levels of both glutaminase and the Slc5a1 (Figure 14H-I). These results confirm that the reduced glucose levels in combination with other changes imposed by STS, have a major effect in down-regulating glycolytic genes and proteins.

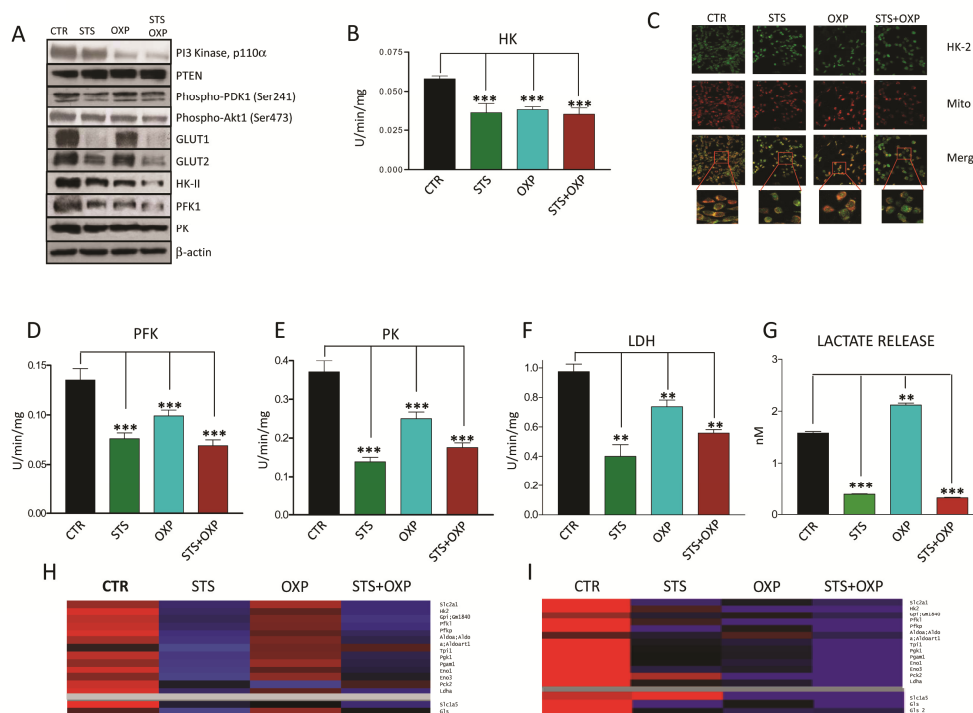


**Figure 14 Effect of STS in combination with chemotherapy on growth and glucose metabolism pathways in colon carcinoma cells.**

CT26 colon carcinoma cells, undergoing STS or incubated under standard conditions and treated with or without 40  $\mu$ M oxaliplatin (OXP) for 24 hours, were lysed and either western blots or enzymatic activities were measured. For protein expression analysis cells were lysed and injected in a nanoscale high-performance liquid chromatography system connected to a hybrid linear trap quadrupole (LTQ) Orbitrap mass spectrometer. Proteins were identified and quantified using MaxQuant pipeline. For gene expression analysis RNA was extracted from CT26 cells and analyzed by microarray hybridization.

Panel A shows the expression of PI3K, PTEN, Phospho-PDK1, Phospho-AKT, GLUT1, GLUT2, HKII, PFK1, PK and  $\beta$ -actin.

Panel B shows the overall activity of HK by CT26 cells.

Panel C shows the confocal microscopy for HK II. After treatment the cells were labeled by MitoTracker Far Red and stained for HK II expression by immunofluorescence. Merged images indicate that STS+OXP causes a significant and selective dislocation of HK II isoform from mitochondrial membrane to the cytosol.

Panel D-E-F show the activity of Phosphofruktokinase (PFK), Pyruvate kinase (PK), Lactate Dehydrogenase (LDH) by CT26 cells, respectively.

Panel G shows the lactate release measured by spectrometry in the supernatants of CT26 cells. Data are expressed as mean values  $\pm$  SD. P value was calculated using unpaired t test with Welch's correction. \*: P<0.05; \*\*: P<0.01; \*\*\*: P<0.001.

Representative expression heat maps of proteins (Panel H) and genes (Panel I) involved in glycolysis and glutaminolysis are shown. Data are expressed as ratios over mean values for the four conditions (STS, OXP, STS+OXP; red = expression above mean, black= expression at mean; blue = expression below mean)

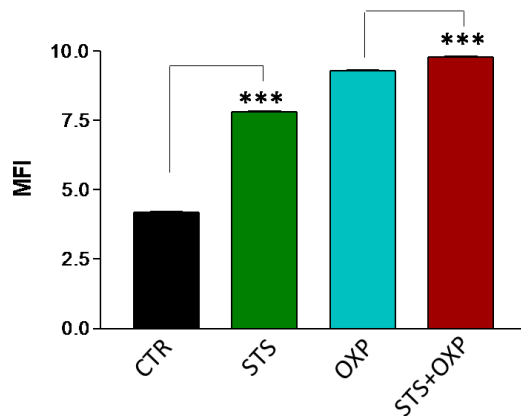


**Figure 15. Effects of starvation in combination with chemotherapy on proliferation of CT26 colon carcinoma cell lines.**

CSFE labeled CT26 colon carcinoma cells were cultured in normal (1.0 g/L glucose + 10% FBS) or starved (0.5 g/L glucose + 1% FBS) conditions 48 hours. Cells were incubated with 40  $\mu$ M oxaliplatin (OXP) for 24 hours. CSFE stained cells were analyzed by cytofluorimetry. MFI = mean fluorescence intensity.

**Starvation and chemotherapy promote uncoupling of the mitochondrial respiratory chain and oxidative stress**

Proteomic and genomic analyses did not show a clear effect of STS in up-regulating OXPHOS although different sets of respiratory enzymes were elevated after STS or OXP or STS+OXP (Figure 16A-B). Clear changes were instead observed when measuring enzymatic activities of respiratory complexes, oxygen consumption and ATP: STS up-regulated Complex I and IV (Figure 17A and C) without affecting Complex II activity (Figure 17B). Consistent with this, a significant increase in O<sub>2</sub> consumption rate (OCR), indicative of an increased oxidative metabolism, was observed (Figure 17D-E). This corresponded to a significant reduction of ATP synthesis (Figure 17F and G). Accordingly, the ATP/AMP ratio, a good indicator of cellular energy charge, was dramatically reduced by the two STS settings (Figure 16C).

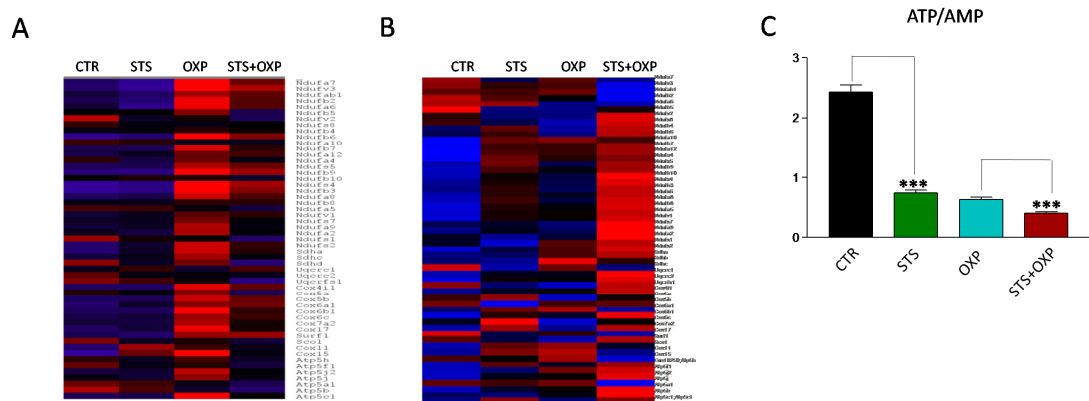


**Figure 16. Expression of oxidative phosphorylation enzymes and energy charge in response to starvation and chemotherapy in colon carcinoma cell lines**

CT26 colon carcinoma cells were starved or not and treated with or without 40  $\mu$ M oxaliplatin (OXP) for 24 hours. For protein expression analysis (Panel A) cells were lysed and injected in nanoscale high-performance liquid chromatography system connected to a hybrid linear trap quadrupole (LTQ) Orbitrap mass spectrometer. Proteins were identified and quantified using



MaxQuant pipeline. For gene expression analysis (Panel B) RNA was extracted from CT26 cells and analyzed by microarray hybridization. Representative expression heatmaps of proteins (Panel A) and genes (Panel B) involved in oxidative phosphorylation are shown. Data are expressed as ratios over mean values for the four conditions (STS, OXP, STS+OXP; red = expression above mean, black = expression at mean; blue = expression below mean)

Panel C shows the ATP/AMP ratio evaluated by spectrometry in CT26, treated with or without STS, OXP or STS + OXP. Data are expressed as the mean value  $\pm$  SD of ATP/AMP ratio.

In order to confirm the stimulatory effect of STS on Complex I-activity, we pre-incubated CT26 cells with Rotenone, a Complex I inhibitor. In the presence of Rotenone, none of the treatments caused a significant OCR increase (Figure 17H) or ATP synthesis reduction (Figure 17I).

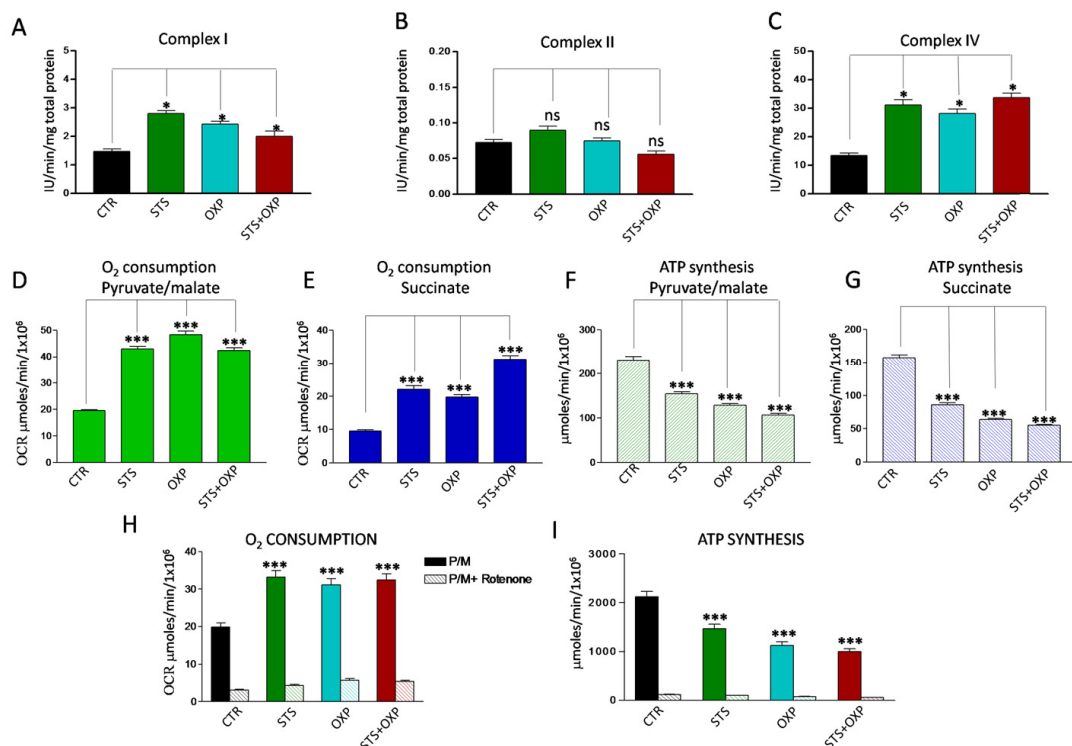


**Figure 17. Effect of STS in combination with chemotherapy on oxidative phosphorylation activity of CT26 colon carcinoma cells.**

Panels A, B and C report the activity of the redox Complexes I, II and IV in CT26 cell lines treated with STS +/- OXP. Data are expressed as mean values  $\pm$  SD. P value was calculated using unpaired t-test with Welch's correction. \*: P<0.05.

Panels D-E show the oxygen consumption rate (OCR) of CT26 in the presence of pyruvate (10mM)/malate (5mM) and succinate (20mM), respectively. OCR was measured by an oxygen micro-respiration electrode and expressed as  $\mu\text{M O}_2/\text{min}/10^6$  cells. Each is representative of at least three experiments.

Panels F-G describe the activity of F0-F1 ATP synthase of CT26 cell lines, measured by luminometric analysis, after the addition of 10 mM pyruvate + 5 mM malate or 20 mM succinate.

Panels H-I show the OCR and ATP synthesis in CT26 cells in the presence of pyruvate (10mM)/malate (5mM) and pre-incubated with Rotenone.

Each is representative of at least six experiments. P value was calculated using unpaired t-test with Welch's correction. \*: P<0.05.

Increased activity of the mitochondrial respiratory chain with a decreased ATP production suggests a possible increase in superoxide generation caused by electron leakage, possibly at complex I and III (127). Indeed, STS and OXP markedly increased ROS generation in CT26 cells and STS+OXP further exacerbated ROS production (Figure 18A). These profound metabolic alterations, characterized by reduced ATP biosynthesis and increased ROS production, are likely responsible for the additive effect of STS+OXP in triggering apoptosis in CT26 cells (Figure 18B-C).

This response was confirmed by proteomic analyses (Figure 18D) documenting an apoptotic signature obtained by hierarchical clustering of a 110 apoptotic proteins (GO:0006915) (128). STS, OXP and especially STS+OXP induced the expression of many pro-apoptotic proteins (Figure

18D). In summary, these results strongly support the effect of STS on reducing glycolysis and lactate production and increasing respiration at Complexes I-IV resulting in superoxide production/oxidative stress but in reduced ATP generation.

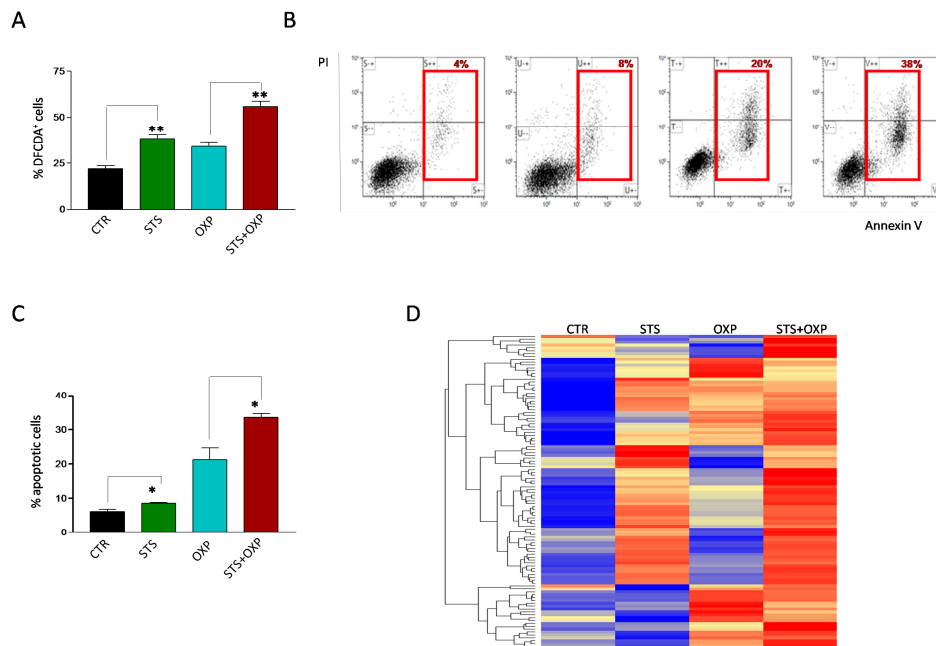


**Figure 18. Effect of STS in combination with chemotherapy on reactive oxygen species production and apoptosis of colon carcinoma cells.**

Panel A shows the oxidation state of the dye Dichlorodihydrofluoresceindiacetate (DCFDA) as a method to assess the level of reactive oxygen species (ROS) in CT26 colon carcinoma cells, undergoing STS (48 hours) or under standard conditions, and treated with or without 100 $\mu$ M oxaliplatin (OXP) for 24 hours. Results are expressed as mean of the percentage of DCFDA positive cells from three different experiments.

Panel B shows a representative dot plot of CT26 cells, undergoing STS or under standard conditions, treated with or without OXP (100 $\mu$ M) and stained with FITC Annexin V and propidium iodide (PI). Red squares indicate the percentage of Annexin<sup>+</sup>/PI<sup>+</sup> and Annexin<sup>+</sup>/PI<sup>+</sup> apoptotic cells (early and late apoptosis).

Panel C shows the percentage of Annexin<sup>+</sup>/PI<sup>-</sup> and Annexin<sup>+</sup>/PI<sup>+</sup> apoptotic CT26 cells expressed as mean value  $\pm$  SD from three different experiments performed. P value was calculated using Unpaired t test with Welch's correction. \*: P<0.05; \*\*: P<0.01.

Panel D shows a representative heat map of proteins annotated by Gene Ontology as involved in apoptosis. Data are expressed as ratios over mean values for the four conditions (STS, OXP, STS+OXP; red = expression above mean, yellow = expression at mean; blue = expression below mean).

## Discussion

Our results indicate that STS, defined as a water only diet lasting 2 days in mice or severe serum plus glucose restriction *in vitro*, causes a profound metabolic shift and promotes an anti-Warburg effect in colon cancer cells. We show that STS *in vitro* down-regulates glycolysis and glutaminolysis and increases OXPHOS and OCR, reduces ATP synthesis and increased ROS production. This latter effect is presumably associated with the induction of apoptosis. Chemotherapy increased this toxicity further by inducing both Complex I and Complex II-dependent respiration, leading to elevated toxic oxygen species generation but reduced ATP generation and death.

Cancer cells alter their metabolism in order to satisfy their bioenergetic and biosynthetic requirements, generating a peculiar metabolic pattern characterized by high anaerobic glycolysis, fatty acid synthesis and glutamine metabolism (11). Aerobic glycolysis produces higher ATP and NADH levels (129, 130) which may contribute to chemoresistance through increased drug efflux from the cell, enhanced DNA repair, dysregulation of growth factor signaling and high expression of survival pathways or anti-apoptotic genes (131). For these reasons, the combination of chemotherapy and agents able to affect the ability of cancer cells to adopt alternate metabolic strategies and survive represents a promising strategy to overcome drug resistance and improve chemotherapeutic index (132). Therapies targeting cancer metabolism such as calorie restriction and ketogenic diet (96, 133) can modify the metabolic state of the whole organism but also that of the tumor cells. Part of the effects of STS can be achieved by agents that target metabolic enzymes including glucose transporters, hexokinase, pyruvate kinase M2, lactate

dehydrogenase, lactate transporter, and glutaminase (111). However, STS provides 2 advantages: 1) in both mice and humans it causes virtually no severe side effects, 2) it affects the function of hundreds of proteins and enzymes thus increasing the chance of affecting a pathway required for tumor cell survival, particularly under the already hostile environment generated by chemotherapy.

Multiple cycles of STS have been shown to protect normal cells against chemotoxicity and to increase the effectiveness of chemotherapeutic drugs against the survival and progression of various tumor types (105, 106). However, whether STS sensitizes tumor cells to chemotherapy by affecting their metabolism is presently unknown. In agreement with previous reports (123, 124, 126), our present results demonstrate that STS, especially in combination with chemotherapy, delays the *in vivo* and *in vitro* growth of colon carcinoma cells. We show that STS significantly reduces cancer glucose consumption leading to a transient arrest in cancer progression followed by a rebound phase after re-feeding. By contrast, STS+OXF causes a more severe metabolic impairment and a long-lasting decrease in cancer growth. Both observations confirm the relationship between glucose consumption and proliferation rate in cancer.

The profound metabolic alterations observed in tumor cells are often related to induction of PI3K-AKT signaling, which plays a pivotal role in glucose metabolism and cancer growth control (11). Phosphorylated AKT has been shown to: i) up-regulate the expression of glucose transporters , ii) enhance glucose capture by HK and iii) to stimulate PFK (109). Our study indicates that STS down-regulates PI3K, AKT, and PDK1 phosphorylation in CT26 colon

carcinoma cells. In contrast, the expression of PTEN, which negatively regulates PI3K-AKT signaling, is significantly induced by STS.

Colon carcinoma cells cultured under starvation conditions exhibit a significant reduction of glucose avidity and consumption. GLUT1, a member of the GLUT (SLC2A) family of membrane transporters that mediates glucose import, is frequently overexpressed in many cancers. Its inhibition can overcome tumor chemoresistance and improve the therapeutic effect of chemodrugs (59, 134, 135). In CT26 cells, glucose intake is known to be mainly dependent on GLUT1 and GLUT2 whose expression levels are dramatically down-regulated by STS. Glucose consumption and the start of the glycolytic process in cancer depends on HK II whose catalytic function is largely empowered by its p-AKT-dependent binding to the outer mitochondrial membrane (136). We show that STS hampers this association which may limit the preferential access of HK II to ATP for glucose-6-phosphate production. STS also limits PFK, PK and LDH activity, which will directly inhibit the rate-limiting steps of glycolytic flux. In addition, STS dramatically reduces the lactate released by CT26 cells, likely due to the concomitant down-regulation of MCT1/Slc16a1 and CD147 (data not shown). The acidification of the tumor microenvironment due to high levels of exported lactate can hamper antitumor immune responses and favor tumor metastasis (137, 14). Also, intracellular lactate may be converted to pyruvate by LDH and used as a nutrient source for oxidative metabolism and/or gluconeogenesis. Marked increase of LDHA, MCT1/4 and CD147 levels correlate with cancer progression and drug resistance (138-140) and the targeting of LDHA and MCT has been proposed as a cancer therapy (141-145). Thus, the effect of STS on glycolysis and lactate production alone, could

cause a major effect on cancer progression, even independently of its effects on mitochondria.

The inhibition of glucose utilization is accompanied by a down-regulatory effect of STS on the glutamine transporters Slc1a5 and glutaminase, which catalyze glutamine catabolism and provide cancer cells with bio-synthetic precursors for aminoacids and DNA synthesis (146, 147). As a metabolic counterpart of glycolysis inhibition, STS induces ROS levels and apoptosis, probably as the result of a futile enhancement of mitochondrial complex activity uncoupled from ATP synthesis. Mitochondrial OXPHOS is the major cellular source of ROS, mainly through the activity of complex I and III. The most likely explanation for the increase in Complex I and IV activities, accompanied by increased OCR but reduced ATP generation and elevated ROS production after STS, OXP or their combination is that the cancer cells are not able to synthesize ATP at the rate dictated by oxygen consumption therefore increasing the electron leakage at Complexes I and III to form superoxide (11, 44, 127) (Figure 19). Higher superoxide and lower ATP could then promotes cell death in part through ROS-induced apoptosis (148, 149, 119). On the other hand, OXP, as a chemotherapeutic agent, provokes DNA damage dependent apoptosis. Hence, the apoptotic activities induced by STS and chemotherapy complement each other. In conclusion, the present study indicates that the combination of STS cycles and chemotherapy causes a major enhancement of chemotherapeutic index, in part by promoting an anti-Warburg effect characterized by reduced glycolysis, reduced lactate generation, and increased oxidative phosphorylation with lower ATP synthesis but higher ROS generation and apoptosis.



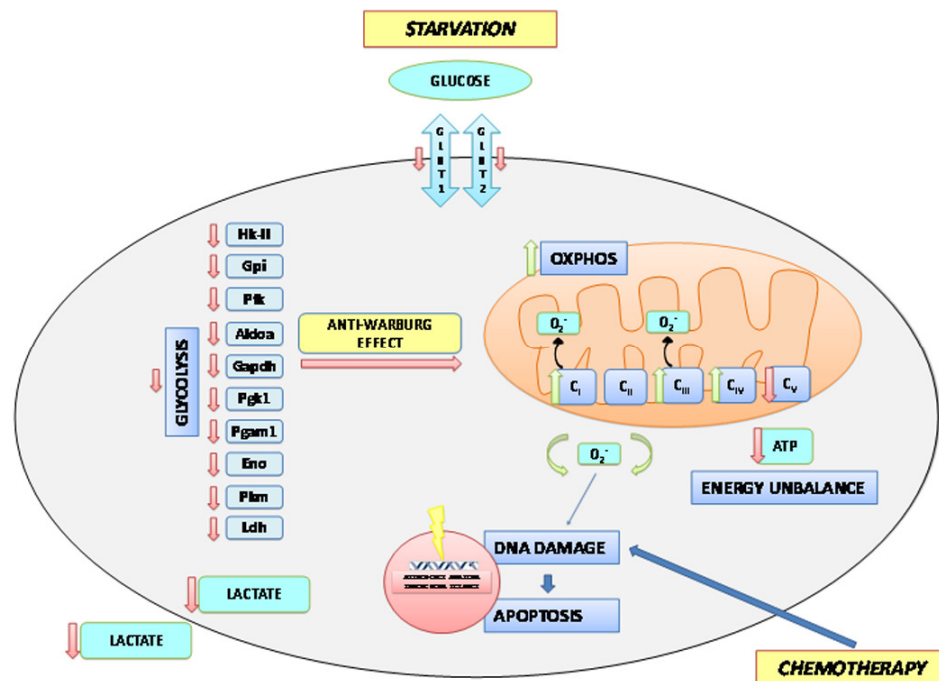


**Figure 19. A Model of Short term starvation effects on the metabolism of the tumor cell**

Starvation in terms of reduced availability of glucose and aminoacids in the extracellular space determines a reduced expression of the glucose transporters Glut1 and Glut2 and leads to a general reduction in the glycolytic rate through the down-regulation of gene and protein expression as well as activity of almost all enzymes of the glycolytic chain. As a consequence, the production and secretion of lactate is reduced, with potential effects on the tumor microenvironment. This anti-Warburg effect is also accompanied by increased activities of complexes I, III and IV of the respiratory chain. However, uncoupling of respiration leads to the production of increased amounts of free oxygen radicals that determine an enhanced oxidative damage to the nuclear DNA. This latter event is responsible for the induction of apoptotic cell death. Uncoupling also causes a reduced activity of complex V of the respiratory chain resulting in ATP deficiency which makes tumor cell more vulnerable to the chemotherapeutic insult.

## **Material and methods**

### **Cell lines and culture conditions**

Tumor cell lines were cultured in DMEM medium (Euroclone, Milan, Italy) supplemented with 1% L-glutamine, penicillin/streptomycin, nonessential amino acids and 10% fetal bovine serum (FBS) (all from Sigma Aldrich, Milan, Italy) (complete medium). All treatments were performed at 37°C under 5% CO<sub>2</sub>. Glucose restriction was done by incubating cells in glucose free DMEM (Invitrogen, Monza, Italy) supplemented with either low glucose (0.5 g/L) or normal glucose (1.0 g/L) for 48 hours. Serum restriction was done by incubating cells in DMEM/F12 with either 10% or 1% FBS for 48 hours. Oxaliplatin (OXP, Hospira, Naples, Italy) treatment was performed 24 hours after STS in a concentration range between 10-100 µM. Optimum drug doses were determined for each individual cell line.

### **Cell viability, proliferation and apoptosis assays**

Colon cancer cell lines were plated in 12-well plates (Falcon, Becton Dickinson, Le Pont de Claix, France) (CT26 and HCT 116  $1 \times 10^5$ , HT-29  $2 \times 10^5$ , cells per well) in complete medium. After 24 hours media were switched to starvation (0.5 g/L glucose + 1% FBS) or control (1 g/L glucose + 10% FBS) and 48 hours later cells were harvested and the number was assessed by Trypan blue (Sigma Aldrich) exclusion. To assess proliferation, cancer cells were labeled with 20µM Carboxyfluorescein Succinimidyl ester (CFSE) (Invitrogen, Milano, Italy) for 15 minutes at 37°C and treated as above described. Then, cells were acquired with a Gallios cytometer.

### **Immunofluorescence analysis**

CT26 cells were incubated with MitoTracker probe (Life Technologies Italia, Monza, Italy) and treated as previously described (150). Coverslips were incubated overnight with rabbit anti-HKI (C35C4) or anti-HKII (C64G5) primary antibodies (Cell Signaling Technologies, Leiden, The Netherlands). Specific staining was visualized with a goat anti-Rabbit Alexa Fluor 488 secondary antibody (Molecular Probe® Life Technology), washed and mounted using Prolong Gold anti-fading reagent (Life Technologies). Results were analyzed using an Olympus (Olympus Optical) laser-scanning microscope FV500 equipped with an Olympus IX81 inverted microscope and Argon ion 488 nm, He-Ne 543 nm, and He-Ne 633 nm lasers. Digital images were acquired through a PLAPO 60× objective, with the Fluoview 4.3b software program, sequentially as single trans-cellular optical sections. Spatial co-localization was analyzed by Image J 1.34f software (NIH).

### **Western blotting**

The antibodies used were as follows: anti-PTEN (Millipore), anti-Phospho-AKT (Ser473), anti-Phospho-PDK1, anti-PI3K, anti-HKII, anti-PFK1, anti-PKM2, anti- $\beta$ -actin (all from Cell Signaling), and anti-GLUT1, GLUT2, GLUT3, GLUT4 (all from Cell Abcam, United Kingdom).

### **Spectrophotometric enzymes assay**

Glycolytic enzymes were assayed at room temperature on 25  $\mu$ g of CT26 cells protein, in a double beam spectrophotometer (UNICAM UV2, Analytical S.n.c., Italy) as previously described (151).

The activity assay of the redox complexes I, II, III, IV was evaluated as described in (152, 153).

ATP and AMP were measured according to the enzyme coupling method described elsewhere (154).

### **Oxygraphic measurements**

O<sub>2</sub> consumption was measured at 25 °C in a closed chamber, using a thermostatically controlled oxygraph apparatus equipped with amperometric electrode (Microrespiration, Unisense A/S, Århus, Denmark) as described (155). In some experiments, CT26 cells were pre-incubated with 50 μM Rotenone (Sigma) 5 minutes before performing O<sub>2</sub> measure.

### **Bioluminescent luciferase ATP assay**

Fifty microrgrams of CT26 cell proteins were incubated in an appropriate buffer plus 5 mM pyruvate and 2.5 mM malate as described in (156) and ATP synthesis was then induced adding 0.1 mM ADP. ATP concentration was measured in a luminometer (Lumi-Scint, Bioscan) by the luciferin/luciferase chemiluminescent method (157). In some experiments, CT26 cells were pre-incubated with 50 μM Rotenone (Sigma) 5 minutes before performing ATP measure. In all experiments the ATP synthesis rate was linear for the first 2 minutes.

### **Proteomic analysis**

The MS instrument was operated in data-dependent mode to automatically switch between full-scan MS and MS/MS acquisition. Survey full-scan MS

spectra were acquired in the Orbitrap analyzer with resolution  $R = 60,000$ . The 20 most intense peptide ions with charge states  $\geq 2$  were sequentially isolated and fragmented by collision-induced dissociation (CID) in the LTQ mass spectrometer. Raw mass spectrometric data were analyzed using the MaxQuant pipeline (158). Moreover quantification and data normalization were achieved by an intensity-based label-free approach using MaxQuant. Thanks to the implementation of maximal peptide ratio extraction and delayed normalization algorithms, the MaxLFQ program included in MaxQuant, provide accurate XIC-based quantification (159). The statistical and the pathways analysis have been made with the freely available Perseus ([www.perseusframework.org/Perseus\\_1.4.1.3.zip](http://www.perseusframework.org/Perseus_1.4.1.3.zip)) and Cytoscape software respectively (160).

### **Microarray**

RNA was extracted from cell lines using RNeasy (Qiagen, Hilden, Germany). RNA quality was assessed in the BioAnalyzer (Agilent, St. Clara, CA). cDNA, ds-cDNA and cRNA synthesis was performed using the 3' IVT Express Kit (Affymetrix, Santa Clara, CA, USA) according to the manufacturer's instructions. cRNAs were purified using the RNeasy Mini Kit (Qiagen), controlled by agarose gel electrophoresis and subjected to fragmentation for 35 min. at 94 °C in fragmentation buffer (40mM Tris-acetate pH 8.1, 100mM CH<sub>3</sub>COOH, 30mM Mg(CH<sub>3</sub>COO)<sub>2</sub>·4H<sub>2</sub>O). Hybridization, washing and staining were performed using the GeneAtlas® Hybridization, Wash, and Stain Kit for 3' IVT Arrays (Affymetrix, St. Clara, CA).

### **Mouse models**

To establish a subcutaneous cancer mouse model, 6 week-old female BALB/c mice were injected subcutaneously in the lower back with 100  $\mu$ L CT26 colon cancer cells resuspended in PBS at a density of  $2 \times 10^6$  cells/mL ( $2 \times 10^5$  cells/mouse). Five days after tumor cell inoculum, when tumors were palpable, the animals were subdivided into four groups: "Controls" (N=7) with tumor and no treatment which were kept under standard conditions for the whole duration of the study; "STS" animals (N=7) that were submitted to 48-hour STS, "OXP" mice (N=7) treated with OXP for 24 hours, "STS+OXP" mice (N=7) submitted to both treatments. At the end of all treatments mice were submitted to micro-PET imaging. STS consisted in a complete food deprivation with free access to water. "STS" mice were individually housed in a clean new cage to reduce cannibalism and were monitored daily for weight loss and general behavior. "OXP" mice were inoculated intraperitoneally (ip) with OXP at 10 mg/Kg and housed in the presence of food. Tumor size was measured by caliper and tumor volume was calculated using the following equation: tumor volume ( $\text{mm}^3$ ) = (length  $\times$  width  $\times$  height)  $\times$   $\pi/6$ , expressing length, width and height in mm.

### **Fluorodeoxyglucose Uptake Evaluation**

Daily quality controls always documented adequate standards and, in particular, a radiochemical purity  $\geq 98\%$ . Labeling was performed by incubating  $10^6$  cells with FDG according to a procedure validated in our laboratory (150, 161). Immediately before the experiment, glucose free medium was added with two mL PBS containing FDG at a concentration of 37 KBq/mL. Tracer

exposure was maintained for 60 minutes at 37°C. Thereafter, the uptake process was stopped by adding 4 ml of PBS before centrifugation at 450 g for 10 minutes. Supernatant was removed and cell pellet re-suspended in 1ml of saline buffer. Free and bound activities were thus simultaneously counted using a Packard Cobra II gamma counter (Packard, Meriden, CT) with a 10% energy window centered at 511KeV. FDG retention was measured as the ratio between bound and total radioactivity. In all cases, the labeling procedure did not affect cell viability as documented by Trypan blue staining.

### **In vivo micro-PET**

Mice were weighted and anesthesia was induced by ip administration of ketamine (100 mg/Kg) (IMALGERE 1000, Milan, Italy) /xylazine (10 mg/kg) (BIO98 Srl, Milan, Italy). Serum glucose level was tested and animals were positioned on the bed of a dedicated micro-PET system (Albira, Carestream Inc, US) whose two-ring configuration permits to cover the whole animal body in a single bed position. A dose of 3-4 MBq of FDG was then injected through a tail vein, soon after start of a list mode acquisition lasting 50 minutes.

### **In vivo image processing.**

PET data were reconstructed using a maximal likelihood expectation maximization method (MLEM). An experienced observer, unaware of the experimental type of analyzed mouse, identified a volume of interest (VOI) in the left ventricular chamber. Then, the computer was asked to plot the time-concentration curve within this VOI throughout the whole acquisition to define tracer input function. Whole body FDG clearance (in ml x min<sup>-1</sup>) was calculated

using the conventional stochastic approach as the ratio between injected dose and integral of input function from 0 to infinity, fitting the last 20 minutes with a mono-exponential function (162). A further VOI was drawn over cancer lesion to measure maximal standardized uptake value (SUV), i.e. the most commonly accepted index of tissue FDG uptake, expressed as the fraction of injected tracer dose normalized for body weight.

Tumor glucose consumption was expressed in  $\text{nM} \times \text{min}^{-1} \times \text{g}^{-1}$  and was estimated in this last VOI according to Gjedde-Patlak (163) graphical analysis by using the routine of a dedicated software (PMOD, Zurich, Switzerland). Briefly, the software utilizes the input function to transform the original tissue activity measurements by fitting the data in each voxel with the slope of the regression line defined by the model. In all cases, lumped constant value was set at 1.

### **Statistical analysis**

The *in vivo* data are presented as mean  $\pm$  standard deviation (SD). For comparison between different groups, the Null hypothesis was tested by a single factor analysis of variance (ANOVA) for multiple groups. Statistical significance was considered for p values  $p < 0.05$ .

For *in vitro* experiments, the statistical significance of differences between experimental and control groups was assessed by Unpaired t test with Welch's correction using GraphPad Prism 3.0 software (GraphPad Software, Inc, El Camino Real, San Diego, CA).



## Bibliography

1. Brown, G. K. Glucose transporters: structure, function and consequences of deficiency. *J Inherit Metab Dis*, *23*: 237-246, 2000.
2. Ward, P. S. and Thompson, C. B. Metabolic reprogramming: a cancer hallmark even warburg did not anticipate. *Cancer Cell*, *21*: 297-308, 2012.
3. Warburg, O. On the origin of cancer cells. *Science*, *123*: 309-314, 1956.
4. Warburg, O. On respiratory impairment in cancer cells. *Science*, *124*: 269-270, 1956.
5. Bustamante, E. and Pedersen, P. L. High aerobic glycolysis of rat hepatoma cells in culture: role of mitochondrial hexokinase. *Proc Natl Acad Sci U S A*, *74*: 3735-3739, 1977.
6. Frezza, C. and Gottlieb, E. Mitochondria in cancer: not just innocent bystanders. *Semin Cancer Biol*, *19*: 4-11, 2009.
7. Weinhouse, S. The Warburg hypothesis fifty years later. *Z Krebsforsch Klin Onkol Cancer Res Clin Oncol*, *87*: 115-126, 1976.
8. Gatenby, R. A. and Gillies, R. J. Why do cancers have high aerobic glycolysis? *Nat Rev Cancer*, *4*: 891-899, 2004.
9. Gillies, R. J., Robey, I., and Gatenby, R. A. Causes and consequences of increased glucose metabolism of cancers. *J Nucl Med*, *49 Suppl 2*: 24S-42S, 2008.
10. Schulze, A. and Harris, A. L. How cancer metabolism is tuned for proliferation and vulnerable to disruption. *Nature*, *491*: 364-373.

11. Vander Heiden, M. G., Cantley, L. C., and Thompson, C. B. Understanding the Warburg effect: the metabolic requirements of cell proliferation. *Science*, *324*: 1029-1033, 2009.
12. Hirschhaeuser, F., Sattler, U. G., and Mueller-Klieser, W. Lactate: a metabolic key player in cancer. *Cancer Res*, *71*: 6921-6925.
13. Husain, Z., Huang, Y., Seth, P., and Sukhatme, V. P. Tumor-derived lactate modifies antitumor immune response: effect on myeloid-derived suppressor cells and NK cells. *J Immunol*, *191*: 1486-1495.
14. Fischer, K., Hoffmann, P., Voelkl, S., Meidenbauer, N., Ammer, J., Edinger, M., Gottfried, E., Schwarz, S., Rothe, G., Hoves, S., Renner, K., Timischl, B., Mackensen, A., Kunz-Schughart, L., Andreesen, R., Krause, S. W., and Kreutz, M. Inhibitory effect of tumor cell-derived lactic acid on human T cells. *Blood*, *109*: 3812-3819, 2007.
15. Cairns, R. A., Harris, I. S., and Mak, T. W. Regulation of cancer cell metabolism. *Nat Rev Cancer*, *11*: 85-95.
16. Jang, M., Kim, S. S., and Lee, J. Cancer cell metabolism: implications for therapeutic targets. *Exp Mol Med*, *45*: e45.
17. Engelman, J. A. Targeting PI3K signalling in cancer: opportunities, challenges and limitations. *Nat Rev Cancer*, *9*: 550-562, 2009.
18. Engelman, J. A., Luo, J., and Cantley, L. C. The evolution of phosphatidylinositol 3-kinases as regulators of growth and metabolism. *Nat Rev Genet*, *7*: 606-619, 2006.
19. Sarbassov, D. D., Guertin, D. A., Ali, S. M., and Sabatini, D. M. Phosphorylation and regulation of Akt/PKB by the rictor-mTOR complex. *Science*, *307*: 1098-1101, 2005.

20. Boulbes, D., Chen, C. H., Shaikenov, T., Agarwal, N. K., Peterson, T. R., Addona, T. A., Keshishian, H., Carr, S. A., Magnuson, M. A., Sabatini, D. M., and Sarbassov dos, D. Rictor phosphorylation on the Thr-1135 site does not require mammalian target of rapamycin complex 2. *Mol Cancer Res*, 8: 896-906.
21. Song, M. S., Salmena, L., and Pandolfi, P. P. The functions and regulation of the PTEN tumour suppressor. *Nat Rev Mol Cell Biol*, 13: 283-296.
22. Vivanco, I. and Sawyers, C. L. The phosphatidylinositol 3-Kinase AKT pathway in human cancer. *Nat Rev Cancer*, 2: 489-501, 2002.
23. Li, J., Simpson, L., Takahashi, M., Miliaresis, C., Myers, M. P., Tonks, N., and Parsons, R. The PTEN/MMAC1 tumor suppressor induces cell death that is rescued by the AKT/protein kinase B oncogene. *Cancer Res*, 58: 5667-5672, 1998.
24. Cardone, M. H., Roy, N., Stennicke, H. R., Salvesen, G. S., Franke, T. F., Stanbridge, E., Frisch, S., and Reed, J. C. Regulation of cell death protease caspase-9 by phosphorylation. *Science*, 282: 1318-1321, 1998.
25. Brunet, A., Bonni, A., Zigmond, M. J., Lin, M. Z., Juo, P., Hu, L. S., Anderson, M. J., Arden, K. C., Blenis, J., and Greenberg, M. E. Akt promotes cell survival by phosphorylating and inhibiting a Forkhead transcription factor. *Cell*, 96: 857-868, 1999.
26. Zhou, B. P., Liao, Y., Xia, W., Zou, Y., Spohn, B., and Hung, M. C. HER-2/neu induces p53 ubiquitination via Akt-mediated MDM2 phosphorylation. *Nat Cell Biol*, 3: 973-982, 2001.

27. Mayo, L. D. and Donner, D. B. A phosphatidylinositol 3-kinase/Akt pathway promotes translocation of Mdm2 from the cytoplasm to the nucleus. *Proc Natl Acad Sci U S A*, 98: 11598-11603, 2001.
28. Vousden, K. H. and Ryan, K. M. p53 and metabolism. *Nat Rev Cancer*, 9: 691-700, 2009.
29. Mathupala, S. P., Heese, C., and Pedersen, P. L. Glucose catabolism in cancer cells. The type II hexokinase promoter contains functionally active response elements for the tumor suppressor p53. *J Biol Chem*, 272: 22776-22780, 1997.
30. Bensaad, K., Tsuruta, A., Selak, M. A., Vidal, M. N., Nakano, K., Bartrons, R., Gottlieb, E., and Vousden, K. H. TIGAR, a p53-inducible regulator of glycolysis and apoptosis. *Cell*, 126: 107-120, 2006.
31. Diehl, J. A., Cheng, M., Roussel, M. F., and Sherr, C. J. Glycogen synthase kinase-3beta regulates cyclin D1 proteolysis and subcellular localization. *Genes Dev*, 12: 3499-3511, 1998.
32. Brunn, G. J., Williams, J., Sabers, C., Wiederrecht, G., Lawrence, J. C., Jr., and Abraham, R. T. Direct inhibition of the signaling functions of the mammalian target of rapamycin by the phosphoinositide 3-kinase inhibitors, wortmannin and LY294002. *Embo J*, 15: 5256-5267, 1996.
33. Rini, B. I. Temsirolimus, an inhibitor of mammalian target of rapamycin. *Clin Cancer Res*, 14: 1286-1290, 2008.
34. Huang, J. and Manning, B. D. The TSC1-TSC2 complex: a molecular switchboard controlling cell growth. *Biochem J*, 412: 179-190, 2008.

35. Barthel, A., Okino, S. T., Liao, J., Nakatani, K., Li, J., Whitlock, J. P., Jr., and Roth, R. A. Regulation of GLUT1 gene transcription by the serine/threonine kinase Akt1. *J Biol Chem*, 274: 20281-20286, 1999.
36. Samih, N., Hovsepian, S., Aouani, A., Lombardo, D., and Fayet, G. Glut-1 translocation in FRTL-5 thyroid cells: role of phosphatidylinositol 3-kinase and N-glycosylation. *Endocrinology*, 141: 4146-4155, 2000.
37. Clarke, J. F., Young, P. W., Yonezawa, K., Kasuga, M., and Holman, G. D. Inhibition of the translocation of GLUT1 and GLUT4 in 3T3-L1 cells by the phosphatidylinositol 3-kinase inhibitor, wortmannin. *Biochem J*, 300 ( Pt 3): 631-635, 1994.
38. Majewski, N., Nogueira, V., Bhaskar, P., Coy, P. E., Skeen, J. E., Gottlob, K., Chandel, N. S., Thompson, C. B., Robey, R. B., and Hay, N. Hexokinase-mitochondria interaction mediated by Akt is required to inhibit apoptosis in the presence or absence of Bax and Bak. *Mol Cell*, 16: 819-830, 2004.
39. Deprez, J., Vertommen, D., Alessi, D. R., Hue, L., and Rider, M. H. Phosphorylation and activation of heart 6-phosphofructo-2-kinase by protein kinase B and other protein kinases of the insulin signaling cascades. *J Biol Chem*, 272: 17269-17275, 1997.
40. Cross, C. E., Halliwell, B., Borish, E. T., Pryor, W. A., Ames, B. N., Saul, R. L., McCord, J. M., and Harman, D. Oxygen radicals and human disease. *Ann Intern Med*, 107: 526-545, 1987.
41. Brown, D. I. and Griendling, K. K. Nox proteins in signal transduction. *Free Radic Biol Med*, 47: 1239-1253, 2009.

42. Jiang, F., Zhang, Y., and Dusting, G. J. NADPH oxidase-mediated redox signaling: roles in cellular stress response, stress tolerance, and tissue repair. *Pharmacol Rev*, *63*: 218-242.
43. Murphy, M. P. How mitochondria produce reactive oxygen species. *Biochem J*, *417*: 1-13, 2009.
44. Brand, M. D. The sites and topology of mitochondrial superoxide production. *Exp Gerontol*, *45*: 466-472.
45. Reczek, C. R. and Chandel, N. S. ROS-dependent signal transduction. *Curr Opin Cell Biol*, *33*: 8-13.
46. Schieber, M. and Chandel, N. S. ROS function in redox signaling and oxidative stress. *Curr Biol*, *24*: R453-462.
47. Nemoto, S. and Finkel, T. Redox regulation of forkhead proteins through a p66shc-dependent signaling pathway. *Science*, *295*: 2450-2452, 2002.
48. Semenza, G. L. Hypoxia-inducible factors: mediators of cancer progression and targets for cancer therapy. *Trends Pharmacol Sci*, *33*: 207-214.
49. Schreck, R., Rieber, P., and Baeuerle, P. A. Reactive oxygen intermediates as apparently widely used messengers in the activation of the NF-kappa B transcription factor and HIV-1. *Embo J*, *10*: 2247-2258, 1991.
50. Blokhina, O., Virolainen, E., and Fagerstedt, K. V. Antioxidants, oxidative damage and oxygen deprivation stress: a review. *Ann Bot*, *91 Spec No*: 179-194, 2003.

51. Fiaschi, T. and Chiarugi, P. Oxidative stress, tumor microenvironment, and metabolic reprogramming: a diabolic liaison. *Int J Cell Biol*, 2012: 762825.
52. Christofk, H. R., Vander Heiden, M. G., Harris, M. H., Ramanathan, A., Gerszten, R. E., Wei, R., Fleming, M. D., Schreiber, S. L., and Cantley, L. C. The M2 splice isoform of pyruvate kinase is important for cancer metabolism and tumour growth. *Nature*, 452: 230-233, 2008.
53. Christofk, H. R., Vander Heiden, M. G., Wu, N., Asara, J. M., and Cantley, L. C. Pyruvate kinase M2 is a phosphotyrosine-binding protein. *Nature*, 452: 181-186, 2008.
54. Hitosugi, T., Kang, S., Vander Heiden, M. G., Chung, T. W., Elf, S., Lythgoe, K., Dong, S., Lonial, S., Wang, X., Chen, G. Z., Xie, J., Gu, T. L., Polakiewicz, R. D., Roesel, J. L., Boggon, T. J., Khuri, F. R., Gilliland, D. G., Cantley, L. C., Kaufman, J., and Chen, J. Tyrosine phosphorylation inhibits PKM2 to promote the Warburg effect and tumor growth. *Sci Signal*, 2: ra73, 2009.
55. Omenn, G. S., Goodman, G. E., Thornquist, M. D., Balmes, J., Cullen, M. R., Glass, A., Keogh, J. P., Meyskens, F. L., Valanis, B., Williams, J. H., Barnhart, S., and Hammar, S. Effects of a combination of beta carotene and vitamin A on lung cancer and cardiovascular disease. *N Engl J Med*, 334: 1150-1155, 1996.
56. Klein, E. A., Thompson, I. M., Jr., Tangen, C. M., Crowley, J. J., Lucia, M. S., Goodman, P. J., Minasian, L. M., Ford, L. G., Parnes, H. L., Gaziano, J. M., Karp, D. D., Lieber, M. M., Walther, P. J., Klotz, L., Parsons, J. K., Chin, J. L., Darke, A. K., Lippman, S. M., Goodman, G.

- E., Meyskens, F. L., Jr., and Baker, L. H. Vitamin E and the risk of prostate cancer: the Selenium and Vitamin E Cancer Prevention Trial (SELECT). *Jama*, *306*: 1549-1556, 2011.
57. Gorrini, C., Harris, I. S., and Mak, T. W. Modulation of oxidative stress as an anticancer strategy. *Nat Rev Drug Discov*, *12*: 931-947.
58. Mueckler, M. and Thorens, B. The SLC2 (GLUT) family of membrane transporters. *Mol Aspects Med*, *34*: 121-138.
59. Chan, D. A., Sutphin, P. D., Nguyen, P., Turcotte, S., Lai, E. W., Banh, A., Reynolds, G. E., Chi, J. T., Wu, J., Solow-Cordero, D. E., Bonnet, M., Flanagan, J. U., Bouley, D. M., Graves, E. E., Denny, W. A., Hay, M. P., and Giaccia, A. J. Targeting GLUT1 and the Warburg effect in renal cell carcinoma by chemical synthetic lethality. *Sci Transl Med*, *3*: 94ra70.
60. Liu, Y., Cao, Y., Zhang, W., Bergmeier, S., Qian, Y., Akbar, H., Colvin, R., Ding, J., Tong, L., Wu, S., Hines, J., and Chen, X. A small-molecule inhibitor of glucose transporter 1 downregulates glycolysis, induces cell-cycle arrest, and inhibits cancer cell growth in vitro and in vivo. *Mol Cancer Ther*, *11*: 1672-1682.
61. Gautier, E. L., Westerterp, M., Bhagwat, N., Cremers, S., Shih, A., Abdel-Wahab, O., Lutjohann, D., Randolph, G. J., Levine, R. L., Tall, A. R., and Yvan-Charvet, L. HDL and Glut1 inhibition reverse a hypermetabolic state in mouse models of myeloproliferative disorders. *J Exp Med*, *210*: 339-353.
62. Christensen, K., Doblhammer, G., Rau, R., and Vaupel, J. W. Ageing populations: the challenges ahead. *Lancet*, *374*: 1196-1208, 2009.



63. Eyre, H., Kahn, R., Robertson, R. M., Clark, N. G., Doyle, C., Hong, Y., Gansler, T., Glynn, T., Smith, R. A., Taubert, K., and Thun, M. J. Preventing cancer, cardiovascular disease, and diabetes: a common agenda for the American Cancer Society, the American Diabetes Association, and the American Heart Association. *Circulation*, *109*: 3244-3255, 2004.
64. Omodei, D. and Fontana, L. Calorie restriction and prevention of age-associated chronic disease. *FEBS Lett*, *585*: 1537-1542.
65. Martin, G. M., Austad, S. N., and Johnson, T. E. Genetic analysis of ageing: role of oxidative damage and environmental stresses. *Nat Genet*, *13*: 25-34, 1996.
66. Poon, H. F., Calabrese, V., Scapagnini, G., and Butterfield, D. A. Free radicals and brain aging. *Clin Geriatr Med*, *20*: 329-359, 2004.
67. Liu, J. and Mori, A. Stress, aging, and brain oxidative damage. *Neurochem Res*, *24*: 1479-1497, 1999.
68. Ames, B. N., Shigenaga, M. K., and Hagen, T. M. Mitochondrial decay in aging. *Biochim Biophys Acta*, *1271*: 165-170, 1995.
69. Longo, V. D. and Finch, C. E. Evolutionary medicine: from dwarf model systems to healthy centenarians? *Science*, *299*: 1342-1346, 2003.
70. Harper, J. M., Salmon, A. B., Chang, Y., Bonkowski, M., Bartke, A., and Miller, R. A. Stress resistance and aging: influence of genes and nutrition. *Mech Ageing Dev*, *127*: 687-694, 2006.
71. Fontana, L., Partridge, L., and Longo, V. D. Extending healthy life span—from yeast to humans. *Science*, *328*: 321-326.

72. Guarente, L. and Kenyon, C. Genetic pathways that regulate ageing in model organisms. *Nature*, *408*: 255-262, 2000.
73. Kenyon, C. A pathway that links reproductive status to lifespan in *Caenorhabditis elegans*. *Ann N Y Acad Sci*, *1204*: 156-162.
74. Rizza, W., Veronese, N., and Fontana, L. What are the roles of calorie restriction and diet quality in promoting healthy longevity? *Ageing Res Rev*, *13*: 38-45.
75. Masoro, E. J. Overview of caloric restriction and ageing. *Mech Ageing Dev*, *126*: 913-922, 2005.
76. Panowski, S. H. and Dillin, A. Signals of youth: endocrine regulation of aging in *Caenorhabditis elegans*. *Trends Endocrinol Metab*, *20*: 259-264, 2009.
77. Mehta, R., Steinkraus, K. A., Sutphin, G. L., Ramos, F. J., Shamieh, L. S., Huh, A., Davis, C., Chandler-Brown, D., and Kaeberlein, M. Proteasomal regulation of the hypoxic response modulates aging in *C. elegans*. *Science*, *324*: 1196-1198, 2009.
78. Piper, M. D., Selman, C., McElwee, J. J., and Partridge, L. Separating cause from effect: how does insulin/IGF signalling control lifespan in worms, flies and mice? *J Intern Med*, *263*: 179-191, 2008.
79. Bartke, A. Minireview: role of the growth hormone/insulin-like growth factor system in mammalian aging. *Endocrinology*, *146*: 3718-3723, 2005.
80. Harrison, D. E., Strong, R., Sharp, Z. D., Nelson, J. F., Astle, C. M., Flurkey, K., Nadon, N. L., Wilkinson, J. E., Frenkel, K., Carter, C. S., Pahor, M., Javors, M. A., Fernandez, E., and Miller, R. A. Rapamycin

fed late in life extends lifespan in genetically heterogeneous mice. *Nature*, 460: 392-395, 2009.

81. Selman, C., Tullet, J. M., Wieser, D., Irvine, E., Lingard, S. J., Choudhury, A. I., Claret, M., Al-Qassab, H., Carmignac, D., Ramadani, F., Woods, A., Robinson, I. C., Schuster, E., Batterham, R. L., Kozma, S. C., Thomas, G., Carling, D., Okkenhaug, K., Thornton, J. M., Partridge, L., Gems, D., and Withers, D. J. Ribosomal protein S6 kinase 1 signaling regulates mammalian life span. *Science*, 326: 140-144, 2009.
82. Longo, V. D. and Fontana, L. Calorie restriction and cancer prevention: metabolic and molecular mechanisms. *Trends Pharmacol Sci*, 31: 89-98.
83. Cohen, E., Paulsson, J. F., Blinder, P., Burstyn-Cohen, T., Du, D., Estepa, G., Adame, A., Pham, H. M., Holzenberger, M., Kelly, J. W., Masliah, E., and Dillin, A. Reduced IGF-1 signaling delays age-associated proteotoxicity in mice. *Cell*, 139: 1157-1169, 2009.
84. Mattson, M. P. Energy intake, meal frequency, and health: a neurobiological perspective. *Annu Rev Nutr*, 25: 237-260, 2005.
85. Colman, R. J., Anderson, R. M., Johnson, S. C., Kastman, E. K., Kosmatka, K. J., Beasley, T. M., Allison, D. B., Cruzen, C., Simmons, H. A., Kemnitz, J. W., and Weindruch, R. Caloric restriction delays disease onset and mortality in rhesus monkeys. *Science*, 325: 201-204, 2009.
86. Willcox, B. J., Willcox, D. C., Todoriki, H., Fujiyoshi, A., Yano, K., He, Q., Curb, J. D., and Suzuki, M. Caloric restriction, the traditional Okinawan diet, and healthy aging: the diet of the world's longest-lived

- people and its potential impact on morbidity and life span. *Ann N Y Acad Sci*, 1114: 434-455, 2007.
87. Walford, R. L., Harris, S. B., and Gunion, M. W. The calorically restricted low-fat nutrient-dense diet in Biosphere 2 significantly lowers blood glucose, total leukocyte count, cholesterol, and blood pressure in humans. *Proc Natl Acad Sci U S A*, 89: 11533-11537, 1992.
  88. Holloszy, J. O. and Fontana, L. Caloric restriction in humans. *Exp Gerontol*, 42: 709-712, 2007.
  89. Fontana, L., Meyer, T. E., Klein, S., and Holloszy, J. O. Long-term calorie restriction is highly effective in reducing the risk for atherosclerosis in humans. *Proc Natl Acad Sci U S A*, 101: 6659-6663, 2004.
  90. Fontana, L., Weiss, E. P., Villareal, D. T., Klein, S., and Holloszy, J. O. Long-term effects of calorie or protein restriction on serum IGF-1 and IGFBP-3 concentration in humans. *Aging Cell*, 7: 681-687, 2008.
  91. Renehan, A. G., Zwahlen, M., Minder, C., O'Dwyer, S. T., Shalet, S. M., and Egger, M. Insulin-like growth factor (IGF)-I, IGF binding protein-3, and cancer risk: systematic review and meta-regression analysis. *Lancet*, 363: 1346-1353, 2004.
  92. Guevara-Aguirre, J., Balasubramanian, P., Guevara-Aguirre, M., Wei, M., Madia, F., Cheng, C. W., Hwang, D., Martin-Montalvo, A., Saavedra, J., Ingles, S., de Cabo, R., Cohen, P., and Longo, V. D. Growth hormone receptor deficiency is associated with a major reduction in pro-aging signaling, cancer, and diabetes in humans. *Sci Transl Med*, 3: 70ra13.

93. Thissen, J. P., Underwood, L. E., and Ketelslegers, J. M. Regulation of insulin-like growth factor-I in starvation and injury. *Nutr Rev*, *57*: 167-176, 1999.
94. Merimee, T. J., Zapf, J., and Froesch, E. R. Insulin-like growth factors in the fed and fasted states. *J Clin Endocrinol Metab*, *55*: 999-1002, 1982.
95. Xie, L., Jiang, Y., Ouyang, P., Chen, J., Doan, H., Herndon, B., Sylvester, J. E., Zhang, K., Molteni, A., Reichle, M., Zhang, R., Haub, M. D., Baybutt, R. C., and Wang, W. Effects of dietary calorie restriction or exercise on the PI3K and Ras signaling pathways in the skin of mice. *J Biol Chem*, *282*: 28025-28035, 2007.
96. Kalaany, N. Y. and Sabatini, D. M. Tumours with PI3K activation are resistant to dietary restriction. *Nature*, *458*: 725-731, 2009.
97. Kim, H. J., Jung, K. J., Yu, B. P., Cho, C. G., Choi, J. S., and Chung, H. Y. Modulation of redox-sensitive transcription factors by calorie restriction during aging. *Mech Ageing Dev*, *123*: 1589-1595, 2002.
98. Chung, K. W., Kim, D. H., Park, M. H., Choi, Y. J., Kim, N. D., Lee, J., Yu, B. P., and Chung, H. Y. Recent advances in calorie restriction research on aging. *Exp Gerontol*, *48*: 1049-1053.
99. Cuervo, A. M., Bergamini, E., Brunk, U. T., Droge, W., Ffrench, M., and Terman, A. Autophagy and aging: the importance of maintaining "clean" cells. *Autophagy*, *1*: 131-140, 2005.
100. Fontana, L. and Klein, S. Aging, adiposity, and calorie restriction. *Jama*, *297*: 986-994, 2007.
101. Hanahan, D. Rethinking the war on cancer. *Lancet*, *383*: 558-563, 2014.

102. Calle, E. E. and Kaaks, R. Overweight, obesity and cancer: epidemiological evidence and proposed mechanisms. *Nat Rev Cancer*, 4: 579-591, 2004.
103. Kershaw, E. E. and Flier, J. S. Adipose tissue as an endocrine organ. *J Clin Endocrinol Metab*, 89: 2548-2556, 2004.
104. Lee, C. and Longo, V. D. Fasting vs dietary restriction in cellular protection and cancer treatment: from model organisms to patients. *Oncogene*, 30: 3305-3316, 2011.
105. Raffaghello, L., Lee, C., Safdie, F. M., Wei, M., Madia, F., Bianchi, G., and Longo, V. D. Starvation-dependent differential stress resistance protects normal but not cancer cells against high-dose chemotherapy. *Proc Natl Acad Sci U S A*, 105: 8215-8220, 2008.
106. Lee, C., Safdie, F. M., Raffaghello, L., Wei, M., Madia, F., Parrella, E., Hwang, D., Cohen, P., Bianchi, G., and Longo, V. D. Reduced levels of IGF-I mediate differential protection of normal and cancer cells in response to fasting and improve chemotherapeutic index. *Cancer Res*, 70: 1564-1572, 2010.
107. Safdie, F. M., Dorff, T., Quinn, D., Fontana, L., Wei, M., Lee, C., Cohen, P., and Longo, V. D. Fasting and cancer treatment in humans: A case series report. *Aging (Albany NY)*, 1: 988-1007, 2009.
108. Raffaghello, L., Safdie, F., Bianchi, G., Dorff, T., Fontana, L., and Longo, V. D. Fasting and differential chemotherapy protection in patients. *Cell Cycle*, 9: 4474-4476.

109. DeBerardinis, R. J., Lum, J. J., Hatzivassiliou, G., and Thompson, C. B. The biology of cancer: metabolic reprogramming fuels cell growth and proliferation. *Cell Metab*, 7: 11-20, 2008.
110. DeBerardinis, R. J., Mancuso, A., Daikhin, E., Nissim, I., Yudkoff, M., Wehrli, S., and Thompson, C. B. Beyond aerobic glycolysis: transformed cells can engage in glutamine metabolism that exceeds the requirement for protein and nucleotide synthesis. *Proc Natl Acad Sci U S A*, 104: 19345-19350, 2007.
111. Zhao, Y., Butler, E. B., and Tan, M. Targeting cellular metabolism to improve cancer therapeutics. *Cell Death Dis*, 4: e532, 2013.
112. Zhou, M., Zhao, Y., Ding, Y., Liu, H., Liu, Z., Fodstad, O., Riker, A. I., Kamarajugadda, S., Lu, J., Owen, L. B., Ledoux, S. P., and Tan, M. Warburg effect in chemosensitivity: targeting lactate dehydrogenase-A re-sensitizes taxol-resistant cancer cells to taxol. *Mol Cancer*, 9: 33, 2010.
113. Tamada, M., Nagano, O., Tateyama, S., Ohmura, M., Yae, T., Ishimoto, T., Sugihara, E., Onishi, N., Yamamoto, T., Yanagawa, H., Suematsu, M., and Saya, H. Modulation of glucose metabolism by CD44 contributes to antioxidant status and drug resistance in cancer cells. *Cancer Res*, 72: 1438-1448, 2012.
114. Tome, M. E., Frye, J. B., Coyle, D. L., Jacobson, E. L., Samulitis, B. K., Dvorak, K., Dorr, R. T., and Briehl, M. M. Lymphoma cells with increased anti-oxidant defenses acquire chemoresistance. *Exp Ther Med*, 3: 845-852, 2012.

115. Nogueira, V. and Hay, N. Molecular pathways: reactive oxygen species homeostasis in cancer cells and implications for cancer therapy. *Clin Cancer Res*, *19*: 4309-4314, 2013.
116. Tennant, D. A., Duran, R. V., and Gottlieb, E. Targeting metabolic transformation for cancer therapy. *Nat Rev Cancer*, *10*: 267-277, 2010.
117. Madhok, B. M., Yeluri, S., Perry, S. L., Hughes, T. A., and Jayne, D. G. Dichloroacetate induces apoptosis and cell-cycle arrest in colorectal cancer cells. *Br J Cancer*, *102*: 1746-1752, 2010.
118. Wise, D. R. and Thompson, C. B. Glutamine addiction: a new therapeutic target in cancer. *Trends Biochem Sci*, *35*: 427-433, 2010.
119. Hamanaka, R. B. and Chandel, N. S. Mitochondrial reactive oxygen species regulate cellular signaling and dictate biological outcomes. *Trends Biochem Sci*, *35*: 505-513, 2010.
120. Brand, M. D., Affourtit, C., Esteves, T. C., Green, K., Lambert, A. J., Miwa, S., Pakay, J. L., and Parker, N. Mitochondrial superoxide: production, biological effects, and activation of uncoupling proteins. *Free Radic Biol Med*, *37*: 755-767, 2004.
121. Trachootham, D., Alexandre, J., and Huang, P. Targeting cancer cells by ROS-mediated mechanisms: a radical therapeutic approach? *Nat Rev Drug Discov*, *8*: 579-591, 2009.
122. Diehn, M., Cho, R. W., Lobo, N. A., Kalisky, T., Dorie, M. J., Kulp, A. N., Qian, D., Lam, J. S., Ailles, L. E., Wong, M., Joshua, B., Kaplan, M. J., Wapnir, I., Dirbas, F. M., Somlo, G., Garberoglio, C., Paz, B., Shen, J., Lau, S. K., Quake, S. R., Brown, J. M., Weissman, I. L., and Clarke, M.



- F. Association of reactive oxygen species levels and radioresistance in cancer stem cells. *Nature*, *458*: 780-783, 2009.
123. Lee, C., Raffaghello, L., Brandhorst, S., Safdie, F. M., Bianchi, G., Martin-Montalvo, A., Pistoia, V., Wei, M., Hwang, S., Merlino, A., Emionite, L., de Cabo, R., and Longo, V. D. Fasting cycles retard growth of tumors and sensitize a range of cancer cell types to chemotherapy. *Sci Transl Med*, *4*: 124ra127, 2012.
124. Safdie, F., Brandhorst, S., Wei, M., Wang, W., Lee, C., Hwang, S., Conti, P. S., Chen, T. C., and Longo, V. D. Fasting enhances the response of glioma to chemo- and radiotherapy. *PLoS One*, *7*: e44603, 2012.
125. Cheng, C. W., Adams, G. B., Perin, L., Wei, M., Zhou, X., Lam, B. S., Da Sacco, S., Mirisola, M., Quinn, D. I., Dorff, T. B., Kopchick, J. J., and Longo, V. D. Prolonged fasting reduces IGF-1/PKA to promote hematopoietic-stem-cell-based regeneration and reverse immunosuppression. *Cell Stem Cell*, *14*: 810-823, 2014.
126. Shi, Y., Felley-Bosco, E., Marti, T. M., Orłowski, K., Pruschy, M., and Stahel, R. A. Starvation-induced activation of ATM/Chk2/p53 signaling sensitizes cancer cells to cisplatin. *BMC Cancer*, *12*: 571, 2012.
127. Venditti, P., Di Stefano, L., and Di Meo, S. Mitochondrial metabolism of reactive oxygen species. *Mitochondrion*, *13*: 71-82, 2013.
128. Dimmer, E. C., Huntley, R. P., Alam-Faruque, Y., Sawford, T., O'Donovan, C., Martin, M. J., Bely, B., Browne, P., Mun Chan, W., Eberhardt, R., Gardner, M., Laiho, K., Legge, D., Magrane, M., Pichler, K., Poggioli, D., Sehra, H., Auchincloss, A., Axelsen, K., Blatter, M. C.,

- Boutet, E., Braconi-Quintaje, S., Breuza, L., Bridge, A., Coudert, E., Estreicher, A., Famiglietti, L., Ferro-Rojas, S., Feuermann, M., Gos, A., Gruaz-Gumowski, N., Hinz, U., Hulo, C., James, J., Jimenez, S., Jungo, F., Keller, G., Lemercier, P., Lieberherr, D., Masson, P., Moinat, M., Pedruzzi, I., Poux, S., Rivoire, C., Roechert, B., Schneider, M., Stutz, A., Sundaram, S., Tognolli, M., Bougueleret, L., Argoud-Puy, G., Cusin, I., Duek-Roggli, P., Xenarios, I., and Apweiler, R. The UniProt-GO Annotation database in 2011. *Nucleic Acids Res*, 40: D565-570, 2012.
129. Fanciulli, M., Bruno, T., Giovannelli, A., Gentile, F. P., Di Padova, M., Rubiu, O., and Floridi, A. Energy metabolism of human LoVo colon carcinoma cells: correlation to drug resistance and influence of lonidamine. *Clin Cancer Res*, 6: 1590-1597, 2000.
130. Zhou, Y., Tozzi, F., Chen, J., Fan, F., Xia, L., Wang, J., Gao, G., Zhang, A., Xia, X., Brasher, H., Widger, W., Ellis, L. M., and Weihua, Z. Intracellular ATP levels are a pivotal determinant of chemoresistance in colon cancer cells. *Cancer Res*, 72: 304-314, 2012.
131. Longley, D. B. and Johnston, P. G. Molecular mechanisms of drug resistance. *J Pathol*, 205: 275-292, 2005.
132. Butler, E. B., Zhao, Y., Munoz-Pinedo, C., Lu, J., and Tan, M. Stalling the engine of resistance: targeting cancer metabolism to overcome therapeutic resistance. *Cancer Res*, 73: 2709-2717, 2013.
133. Champ, C. E., Palmer, J. D., Volek, J. S., Werner-Wasik, M., Andrews, D. W., Evans, J. J., Glass, J., Kim, L., and Shi, W. Targeting metabolism with a ketogenic diet during the treatment of glioblastoma multiforme. *J Neurooncol*, 117: 125-131, 2014.

134. Cao, X., Fang, L., Gibbs, S., Huang, Y., Dai, Z., Wen, P., Zheng, X., Sadee, W., and Sun, D. Glucose uptake inhibitor sensitizes cancer cells to daunorubicin and overcomes drug resistance in hypoxia. *Cancer Chemother Pharmacol*, *59*: 495-505, 2007.
135. Liu, R., Li, H., Liu, L., Yu, J., and Ren, X. Fibroblast activation protein: A potential therapeutic target in cancer. *Cancer Biol Ther*, *13*: 123-129, 2012.
136. Robey, R. B. and Hay, N. Mitochondrial hexokinases, novel mediators of the antiapoptotic effects of growth factors and Akt. *Oncogene*, *25*: 4683-4696, 2006.
137. Swietach, P., Vaughan-Jones, R. D., and Harris, A. L. Regulation of tumor pH and the role of carbonic anhydrase 9. *Cancer Metastasis Rev*, *26*: 299-310, 2007.
138. Hao, J., Chen, H., Madigan, M. C., Cozzi, P. J., Beretov, J., Xiao, W., Delprado, W. J., Russell, P. J., and Li, Y. Co-expression of CD147 (EMMPRIN), CD44v3-10, MDR1 and monocarboxylate transporters is associated with prostate cancer drug resistance and progression. *Br J Cancer*, *103*: 1008-1018, 2010.
139. Chen, H., Wang, L., Beretov, J., Hao, J., Xiao, W., and Li, Y. Co-expression of CD147/EMMPRIN with monocarboxylate transporters and multiple drug resistance proteins is associated with epithelial ovarian cancer progression. *Clin Exp Metastasis*, *27*: 557-569, 2010.
140. Kang, M. J., Kim, H. P., Lee, K. S., Yoo, Y. D., Kwon, Y. T., Kim, K. M., Kim, T. Y., and Yi, E. C. Proteomic analysis reveals that

CD147/EMMPRIN confers chemoresistance in cancer stem cell-like cells. *Proteomics*, *13*: 1714-1725, 2013.

141. Fang, J., Quinones, Q. J., Holman, T. L., Morowitz, M. J., Wang, Q., Zhao, H., Sivo, F., Maris, J. M., and Wahl, M. L. The H<sup>+</sup>-linked monocarboxylate transporter (MCT1/SLC16A1): a potential therapeutic target for high-risk neuroblastoma. *Mol Pharmacol*, *70*: 2108-2115, 2006.
142. Gerlinger, M., Santos, C. R., Spencer-Dene, B., Martinez, P., Endesfelder, D., Burrell, R. A., Vetter, M., Jiang, M., Saunders, R. E., Kelly, G., Dykema, K., Rioux-Leclercq, N., Stamp, G., Patard, J. J., Larkin, J., Howell, M., and Swanton, C. Genome-wide RNA interference analysis of renal carcinoma survival regulators identifies MCT4 as a Warburg effect metabolic target. *J Pathol*, *227*: 146-156, 2012.
143. Doherty, J. R., Yang, C., Scott, K. E., Cameron, M. D., Fallahi, M., Li, W., Hall, M. A., Amelio, A. L., Mishra, J. K., Li, F., Tortosa, M., Genau, H. M., Rounbehler, R. J., Lu, Y., Dang, C. V., Kumar, K. G., Butler, A. A., Bannister, T. D., Hooper, A. T., Unsal-Kacmaz, K., Roush, W. R., and Cleveland, J. L. Blocking Lactate Export by Inhibiting the Myc Target MCT1 Disables Glycolysis and Glutathione Synthesis. *Cancer Res*, *74*: 908-920, 2014.
144. Le Floch, R., Chiche, J., Marchiq, I., Naiken, T., Ilc, K., Murray, C. M., Critchlow, S. E., Roux, D., Simon, M. P., and Pouyssegur, J. CD147 subunit of lactate/H<sup>+</sup> symporters MCT1 and hypoxia-inducible MCT4 is critical for energetics and growth of glycolytic tumors. *Proc Natl Acad Sci U S A*, *108*: 16663-16668, 2011.

145. Baba, M., Inoue, M., Itoh, K., and Nishizawa, Y. Blocking CD147 induces cell death in cancer cells through impairment of glycolytic energy metabolism. *Biochem Biophys Res Commun*, 374: 111-116, 2008.
146. Todorova, V. K., Kaufmann, Y., Luo, S., and Klimberg, V. S. Tamoxifen and raloxifene suppress the proliferation of estrogen receptor-negative cells through inhibition of glutamine uptake. *Cancer Chemother Pharmacol*, 67: 285-291, 2011.
147. Karunakaran, S., Ramachandran, S., Coothankandaswamy, V., Elangovan, S., Babu, E., Periyasamy-Thandavan, S., Gurav, A., Gnanaprakasam, J. P., Singh, N., Schoenlein, P. V., Prasad, P. D., Thangaraju, M., and Ganapathy, V. SLC6A14 (ATB0,+) protein, a highly concentrative and broad specific amino acid transporter, is a novel and effective drug target for treatment of estrogen receptor-positive breast cancer. *J Biol Chem*, 286: 31830-31838, 2011.
148. Brenner, C. and Grimm, S. The permeability transition pore complex in cancer cell death. *Oncogene*, 25: 4744-4756, 2006.
149. Kamata, H., Honda, S., Maeda, S., Chang, L., Hirata, H., and Karin, M. Reactive oxygen species promote TNF $\alpha$ -induced death and sustained JNK activation by inhibiting MAP kinase phosphatases. *Cell*, 120: 649-661, 2005.
150. Salani, B., Marini, C., Rio, A. D., Ravera, S., Massollo, M., Orengo, A. M., Amaro, A., Passalacqua, M., Maffioli, S., Pfeffer, U., Cordera, R., Maggi, D., and Sambuceti, G. Metformin impairs glucose consumption

- and survival in Calu-1 cells by direct inhibition of hexokinase-II. *Sci Rep*, 3: 2070, 2013.
151. Ravera, S., Bartolucci, M., Calzia, D., Aluigi, M. G., Ramoino, P., Morelli, A., and Panfoli, I. Tricarboxylic acid cycle-sustained oxidative phosphorylation in isolated myelin vesicles. *Biochimie*, 95: 1991-1998, 2013.
  152. Sottocasa, G. L., Kuylenstierna, B., Ernster, L., and Bergstrand, A. An electron-transport system associated with the outer membrane of liver mitochondria. A biochemical and morphological study. *J Cell Biol*, 32: 415-438, 1967.
  153. Baracca, A., Sgarbi, G., Solaini, G., and Lenaz, G. Rhodamine 123 as a probe of mitochondrial membrane potential: evaluation of proton flux through F(0) during ATP synthesis. *Biochim Biophys Acta*, 1606: 137-146, 2003.
  154. Ravera, S., Vaccaro, D., Cuccarolo, P., Columbaro, M., Capanni, C., Bartolucci, M., Panfoli, I., Morelli, A., Dufour, C., Cappelli, E., and Degan, P. Mitochondrial respiratory chain Complex I defects in Fanconi anemia complementation group A. *Biochimie*, 95: 1828-1837.
  155. Ravera, S., Panfoli, I., Calzia, D., Aluigi, M. G., Bianchini, P., Diaspro, A., Mancardi, G., and Morelli, A. Evidence for aerobic ATP synthesis in isolated myelin vesicles. *Int J Biochem Cell Biol*, 41: 1581-1591, 2009.
  156. Ravera, S., Panfoli, I., Aluigi, M. G., Calzia, D., and Morelli, A. Characterization of Myelin Sheath F(o)F(1)-ATP synthase and its regulation by IF(1). *Cell Biochem Biophys*, 59: 63-70, 2011.

157. Ravera, S., Aluigi, M. G., Calzia, D., Ramoino, P., Morelli, A., and Panfoli, I. Evidence for ectopic aerobic ATP production on C6 glioma cell plasma membrane. *Cell Mol Neurobiol*, *31*: 313-321, 2011.
158. Cox, J. and Mann, M. MaxQuant enables high peptide identification rates, individualized p.p.b.-range mass accuracies and proteome-wide protein quantification. *Nat Biotechnol*, *26*: 1367-1372, 2008.
159. Cox, J., Hein, M. Y., Lubner, C. A., Paron, I., Nagaraj, N., and Mann, M. Accurate proteome-wide label-free quantification by delayed normalization and maximal peptide ratio extraction, termed MaxLFQ. *Mol Cell Proteomics*, *13*: 2513-2526, 2014.
160. Cline, M. S., Smoot, M., Cerami, E., Kuchinsky, A., Landys, N., Workman, C., Christmas, R., Avila-Campilo, I., Creech, M., Gross, B., Hanspers, K., Isserlin, R., Kelley, R., Killcoyne, S., Lotia, S., Maere, S., Morris, J., Ono, K., Pavlovic, V., Pico, A. R., Vailaya, A., Wang, P. L., Adler, A., Conklin, B. R., Hood, L., Kuiper, M., Sander, C., Schmulevich, I., Schwikowski, B., Warner, G. J., Ideker, T., and Bader, G. D. Integration of biological networks and gene expression data using Cytoscape. *Nat Protoc*, *2*: 2366-2382, 2007.
161. Wurth, R., Pattarozzi, A., Gatti, M., Bajetto, A., Corsaro, A., Parodi, A., Sirito, R., Massollo, M., Marini, C., Zona, G., Fenoglio, D., Sambucetti, G., Filaci, G., Daga, A., Barbieri, F., and Florio, T. Metformin selectively affects human glioblastoma tumor-initiating cell viability: A role for metformin-induced inhibition of Akt. *Cell Cycle*, *12*: 145-156, 2013.
162. Iozzo, P., Gastaldelli, A., Jarvisalo, M. J., Kiss, J., Borra, R., Buzzigoli, E., Viljanen, A., Naum, G., Viljanen, T., Oikonen, V., Knuuti, J.,

- Savunen, T., Salvadori, P. A., Ferrannini, E., and Nuutila, P. 18F-FDG assessment of glucose disposal and production rates during fasting and insulin stimulation: a validation study. *J Nucl Med*, 47: 1016-1022, 2006.
163. Patlak, C. S., Blasberg, R. G., and Fenstermacher, J. D. Graphical evaluation of blood-to-brain transfer constants from multiple-time uptake data. *J Cereb Blood Flow Metab*, 3: 1-7, 1983.



## **Ringraziamenti.**

Ringrazio il Dr. Vito Pistoia, primario del Laboratorio di Oncologia del Gaslini di Genova, per avermi dato la possibilità di lavorare per lui e con lui, sin dall'inizio del mio percorso nel mondo della ricerca iniziato 10 anni fa.

Ringrazio la Dr.ssa Lizzia Raffaghello, mia tutor e soprattutto mia amica. A lei devo tutto quello che so e oltre.

Ringrazio la mia relatrice, la Prof.ssa Maria Adelaide Pronzato.

In fine, ma non per importanza, ringrazio tutte le persone che mi vogliono bene e che fanno sì che la mia vita sia una tavolozza di colori.

# INDEX

|   |       |
|---|-------|
| <b>Background</b>   | Pag3  |
| • Cellular metabolism   | Pag3  |
| • <u>The Warburg effect</u>   | Pag5  |
| • <u>The PI3K/ATK/mTOR pathway</u>  | Pag8  |
| • <u>ROS: a double edge sword</u>   | Pag11 |
| • <u>Targeting the Warburg effect to treat cancer</u>   | Pag16 |
| <br>  |       |
| <b>Calorie restriction</b>  | Pag17 |
| • <u>Definition</u>   | Pag17 |
| • <u>Calorie restriction in model organism</u>  | Pag19 |
| • <u>Calorie restriction in humans</u>  | Pag22 |
| • <u>Calorie restriction: molecular and metabolic aspects</u>   | Pag23 |
| • <u>Short-term-starvation, differential-stress-resistance and cancer</u>   | Pag25 |
| <br>  |       |
| <b>Summary of the study</b>   | Pag29 |
| <br>  |       |
| <b>Introduction</b>   | Pag30 |
| <br>  |       |
| <b>Results</b>  | Pag31 |
| • <u>Effects of fasting cycles and chemotherapy on colon carcinoma growth and glucose consumption in vivo</u>             | Pag31 |
| • <u>In vitro effects of STS and chemotherapy on viability and metabolism of colon carcinoma cells</u>                    | Pag34 |
| • <u>Starvation and chemotherapy differentially regulate proliferation and metabolic enzymes in colon carcinoma cells</u> | Pag34 |
| • <u>Expression of glycolytic and glutaminolytic enzymes in response to STS and chemotherapy</u>                          | Pag37 |
| • <u>Starvation and chemotherapy promote uncoupling of the mitochondrial respiratory chain and oxidative stress</u>       | Pag40 |
| <br>  |       |
| <b>Discussion</b>   | Pag45 |
| <br>  |       |
| <b>Material and methods</b>   | Pag50 |
| • <u>Cell lines and culture conditions</u>  | Pag50 |
| • <u>Cell viability, proliferation and apoptosis assays</u>   | Pag50 |
| • <u>Immunofluorescence analysis</u>  | Pag51 |
| • <u>Western blotting</u>   | Pag51 |
| • <u>Spectrophotometric enzymes assay</u>   | Pag51 |
| • <u>Oxygraphic measurements</u>  | Pag52 |
| • <u>Bioluminescent luciferase ATP assay</u>  | Pag52 |
| • <u>Proteomic analysis</u>   | Pag52 |
| • <u>Microarray</u>   | Pag53 |
| • <u>Mouse models</u>   | Pag54 |
| • <u>Fluorodeoxyglucose Uptake Evaluation</u>   | Pag54 |
| • <u>In vivo micro-PET</u>  | Pag55 |
| • <u>In vivo image processing</u>   | Pag55 |
| • <u>Statistical analysis</u>   | Pag56 |
| <br>  |       |
| <b>Bibliography</b>   | Pag57 |
| <br>  |       |
| <b>Acknowledgements</b>   | Pag81 |

